AD NUMBER

ADA173988

NEW LIMITATION CHANGE

TO
Approved for public release, distribution
unlimited

FROM
Distribution authorized to U.S. Gov't.
agencies and their contractors;
Administrative/Operational use; Oct 1986.
Other requests shall be referred to
Defense Advanced Research Projects Agency,
Arlington VA 22022-0000.

AUTHORITY

ONR ltr date Oct 29 1986

AD-A173 988

ADVANCED RESEARCH PROJECTS AGENCY

TECHNICAL REPORT NO. 1 (October 1986)

"The Reactivity of Carboxylic Acid and Ester Groups in the Functionalized
Interfacial Region of "Polyethylene Carboxylic Acid" (PE-CO$_2$H) and
Derivatives: Differentiation of the Functional Groups into Shallow and Deep
Subsets Based on a Comparison of Contact Angle and ATR-IR Measurements"

by Stephen Randall Holmes-Farley and George M. Whitesides

Accepted for publication in <u>Langmuir</u>

DTIC
ELECTE
NOV 3 1986

A

The views and conclusions contained in this document are those of the authors
and should not be interpreted as necessarily representing the official
policies, either expressed or implied, of the Defense Advanced Research
Projects Agency or the U.S. Government.

The Reactivity of Carboxylic Acid and Ester Groups in the Functionalized

Interfacial Region of "Polyethylene Carboxylic Acid" (PE-CO$_2$H) and

Derivatives: Differentiation of the Functional Groups into Shallow and Deep

Subsets based on a Comparison of Contact Angle and ATR-IR Measurements[1]

Stephen Randall Holmes-Farley[2] and George M. Whitesides*

Department of Chemistry

Harvard University

Cambridge, MA   02138

This report is complete per Ms. Giselle Weiss, Harvard University, Dept. of Chemistry

have been differentiated

Abstract. We have differentiated the carboxylic acid groups present in the

functionalized interface of "polyethylene carboxylic acid" (PE-CO$_2$H, a

material prepared from low-density polyethylene film by reaction with aqueous

chromic acid) into two subsets: those sufficiently close to the surface of

the polymer to influence its wettability by water and those too deep to do

so. This differentiation was accomplished by taking advantage of differences

in rates of esterification of carboxylic acid groups in different regions of

the functionalized interface, and of differences in rates of hydrolysis of

ester groups derived from them. The subset of functional groups influencing

wettability comprises <30% of the total groups present in the functionalized

interface and appears to be homogeneous in its chemical reactivity. The

remaining groups (~70% of the total) do not directly influence wettability and

appear to become less reactive with increasing depth in the polymer. The

surface and subsurface carboxylic acid and ester moieties are both less

reactive in hydrolysis and formation reactions than are these groups in

organic molecules in solution. Reactivities of the interfacial functional groups depend on structure in ways having no analogy in reactions in solution. For example, the rate of base-catalyzed hydrolysis of esters present in the functionalized polymer interface is a strong function of the length of the alcohol component of the ester: n-octyl esters are more than 20,000 times less reactive than methyl esters. We have also explored the acidity of the interfacial carboxylic acid groups using ATR-IR spectroscopy and contact angle measurements as probes. Both the local polarity of the environment of individual carboxylic acid groups and charge-charge interactions between carboxylate anions appear to be important in determining acidity. Comparisons of wettability of samples containing different proportions of carboxylic acid, carboxylate anion and ester groups indicates that wettability is particularly sensitive to low concentrations of carboxylate anion. We hypothesize that this sensitivity reflects a limited ability of the functionalized interfacial region to reconstruct--perhaps only by small-amplitude rotations of its constituent carboxylate ions--in a way that minimizes its free energy by maximizing the number of these hydrophilic moieties in direct contact with the polar, aqueous liquid phase.

Introduction

Treatment of low-density polyethylene film with aqueous chromic acid solution under conditions defined previously introduces carboxylic acid moieties into a thin interfacial region on the surface of the film.[3-6] We are developing the chemistry of this material--"polyethylene carboxylic acid" (PE-CO$_2$H)--as a model substrate with which to study the physical-organic chemistry of organic surfaces. Previous studies have demonstrated that the only significant functional groups present in PE-CO$_2$H are carboxylic acid

($\sim$60%) and ketone and/or aldehyde (40%) moieties.[3,5] We have not established the detailed spatial distribution of these functional groups in the polymer, but emphasize that all of them can be titrated with aqueous base, and are thus accessible to hydroxide ion in aqueous solution.[3]

This paper establishes that it is possible to separate the carboxylic acid functionalities in PE-CO$_2$H into two functionally distinct groups: those lying at, or very close to, the surface of the polymer and influencing the wetting of PE-CO$_2$H by aqueous solutions, and those lying deeper in the functionalized interfacial region and having no apparent influence on wetting. The evidence for the existence of "surface" and "subsurface" functional groups--and by inference, for the existence of a functionalized region of finite thickness on the polymer surface--is based on comparisons of data obtained using experimental techniques having different degrees of surface sensitivity. These techniques include contact angle measurements, which respond to the functional groups in direct contact with the liquid phase; ESCA, which observes a thin ($\sim$5 nm) outer layer of the interface including the functional groups that determine the wettability of the surface; and ATR-IR and fluorescence spectroscopy, which detect all of the functional groups in a thick layer of surface (>1000 nm). Here we demonstrate that it is possible to obtain complete conversion of the carboxylic acid groups that influence contact angle to ester groups while converting only approximately 30% of the carboxylic acid groups detectable by ATR-IR spectroscopy. We infer from this comparison that $\sim$30% of the carboxylic acid groups in the oxidized interfacial region of PE-CO$_2$H are "surface" groups, and that $\sim$70% are "subsurface" groups.

We point out explicitly that this distinction between "surface" and "subsurface" functionality is a matter of definition and experimental

technology. In this work, we equate the terms "surface groups" and "groups capable of interacting sufficiently with a contacting fluid to influence the contact angle." This defined equivalence and the underlying assumption that only a group in (on) the surface of the $PE-CO_2H$ is able to influence wetting of this solid is intuitively reasonable but qualitative. The theory of and experimental basis for studying wetting are not highly developed for complex, amorphous, structurally unstable surfaces of the type presented by $PE-CO_2H$. In particular, current treatments of wetting[7-23] do not help to resolve three ambiguities (illustrated schematically in Figure 1). The first (A) is the question of the distance of a functional group influencing contact angle from the surface. For a hypothetical, uniform, planar solid, how close must a functional group be to a contacting liquid phase to influence the wetting behavior of the surface? The second (B) concerns surface microtopology. What will be the influence of the functional group of interest when placed in declivities in the surface? How will the shape of these declivities influence wetting? The third and most difficult (C) concerns the rationalization of real substrate-solvent interfaces. How will the influence of the functional group of interest vary with its position within the solvent-swollen surface layer, and with the structure of this layer? How important is surface reconstruction that changes the position of this functional group in determining the free energy of the interface? How rapidly does the system of substrate and liquid reach thermodynamic equilibrium, and how much of observed wetting phenomena reflect kinetic rather than thermodynamic factors? Current experimental evidence suggests that the distance from the surface over which a subsurface functional group can exercise an influence on wetting (Figure 1A) is small[24]--that is, the functional group must be in direct van der Waals contact with the liquid phase, or separated from it by no more than a few Å,
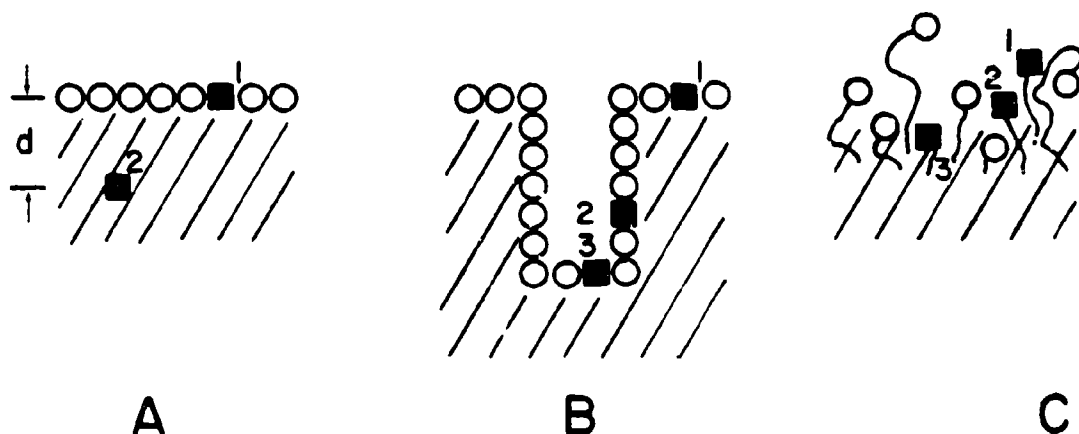
Figure 1. Ambiguities concerning influence of a functional group of (■) on wetting. A: On the surface (position 1) and in the interior of a planar solid (position 2). B: On the surface (1), on the wall (2) and at the bottom of a microcrack (3). C: In the outmost (1), middle (2) and base (3) of a solvent-swollen surface gel region.

to influence wetting. There is currently little evidence bearing on problems in surface microtopology or in the behavior of solvent-swollen surface layers or surface gels, although theoretical studies of certain limiting problems in surface topol⋅ the ∿1 μm scale are available.[9,10,20,22]

Nomenclat⋅ The objective of this work is to study the functionalized interfacial region (the interphase) between PE-CO$_2$H and its derivatives and water. This study is complicated from several points of view, among which is that of the proper nomenclature to use in describing the distribution and reactivity of functionality in a polyfunctional, structurally heterogeneous, three-dimensional solid.

We divide the interphase into three regions. The first is the outermost: that which most closely corresponds to a "surface." This region is that examined by using the most surface-sensitive technique at our disposal--measurement of wetting using contact angles. The second region is the "near surface" region. Groups in this region (together with those in the outermost) can be examined by surface-selective instrumental techniques such as ESCA.[4] The third region comprises the deeper regions of the polymer. Groups in this region can be detected using infrared,[3-6] visible, fluorescence,[4,6] and ESR spectroscopy,[6] but are unlikely to influence surface properties. They are, nonetheless, important in studies of surface chemistry as a source of, or sink for, surface functionality during surface reconstruction.

The major analytical distinction on which this work is based is the identification of the subset of functional groups in the interphase that determine the contact angle of water with the substrate (the "shallow" or "surface" subset); the remaining functional groups present in the interphase

comprise the "deep" or "subsurface" subset. Each of these two subsets may, of course, contain several different types of functional groups. The nomenclature we propose to use is illustrated in Figure 2. We refer to the different sets of functional groups present in the interphase primarily by reference to the analytical technique sensitive to that region. Those groups that influence wetting behavior will be referred to as occupying the "contact angle interphase." Ambiguities in the depth to which the liquid interacts with varied functional groups or groups present in a molecularly rough or solvent-swollen interphase make it impossible at present to define a precise thickness for the contact angle interphase, but on the basis of experiments with ordered organic monolayer films, we believe that for an interphase that is relatively unswollen by the contacting liquid, this thickness is less than 1 nm.[24] Functional groups present in the contact angle interphase are indicated to the right of the vertical line in the symbol ⌐ (a reverse sigma used to represent the "surface"). Groups present in the region sensed by ESCA or Auger (the surface selective spectroscopies) but not present in the contact angle interphase, together with those groups detected by more deeply penetrating forms of spectroscopy (ATR-IR, fluorescence, ESR) and believed for other reasons to be in this same near-surface region will be placed to the left of this vertical line of the symbol ⌐ and under the horizontal bar. For example, PE⌐CO_2CH_3|CO_2H represents polyethylene film having CO_2H groups as the dominant functionality in the contact angle interphase and CO_2CH_3 groups as the major functionality in the sub-contact angle interphase.

The depth of the sub-contact angle interphase depends upon the details of the experiment performed--especially the energy of the emitted photoelectrons in ESCA spectroscopy, and the geometry of the sample relative to the detector. The set of functional groups included in the ESCA interphase
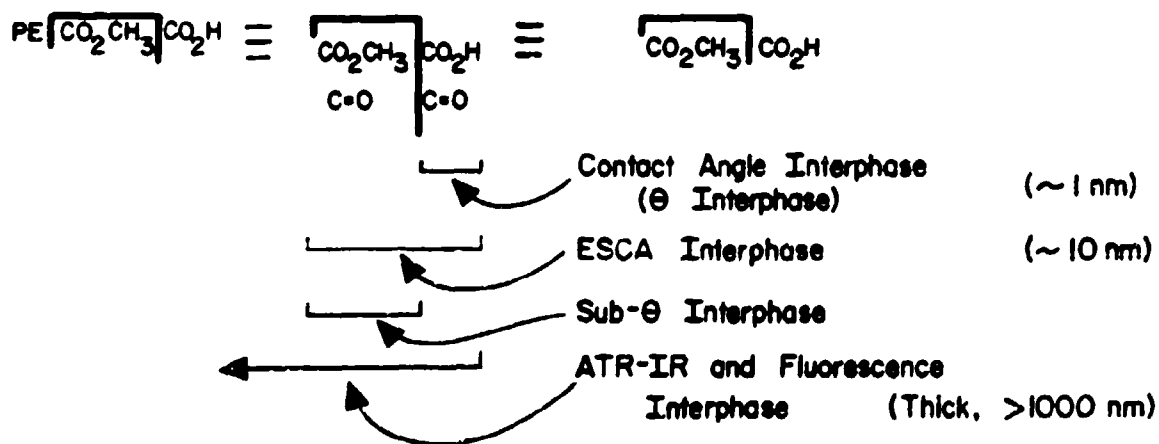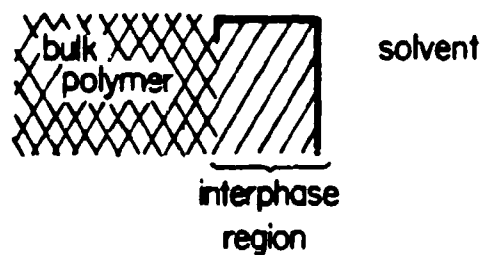
Figure 2. Nomenclature used to describe the several interphase regions of PE-CO₂H and its derivatives.

includes (and may, in fact, be dominated by) those groups present in the contact angle interphase. Groups specifically identified as lying beyond the viewing depth of ESCA spectroscopy but detected by the surface insensitive spectroscopies will be placed to the left of the symbol ⅂.

We abbreviate the phrase "contact angle interphase" by "θ interphase." We emphasize that the requirement that certain spectroscopies must be conducted in high vacuum while other surface probes tolerate or require contact with liquid makes it probable that measurements using different techniques do not see the same sample, but rather a common starting material more or less strongly influenced by interaction with solvent and other features of its environment.

Experimental Methods and Treatment of Data. Much of this paper is based on following the interconversion of carboxylic acid and carboxylic ester moieties on PE-CO$_2$H (PE-CO$_2$R) by two techniques--ATR-IR spectroscopy and measurement of contact angle--and comparing results from these two techniques to differentiate processes occurring throughout the functionalized interface (ATR-IR) from those occurring in the surface (contact angle).

ATR-IR mesasurements were based on following the disappearance of the absorption due to carboxylate anion (CO$_2^-$) in samples that had been made basic, since the peaks due to carboxylic acid (CO$_2$H), methyl ester, and ketone/aldehyde groups overlap.[3,4] The experimental procedure used to measure these IR spectra involved equilibrating the sample with aqueous base (0.1 N NaOH), removing the excess aqueous solution by blotting the surface of the polymer with filter paper, and pressing the resulting (superficially dry) sample against the ATR-IR plate. Control experiments established that contact of the samples with the strong base (pH 13) used in these equilibrations did

not influence the extent of esterification: that is, base-catalyzed hydrolysis was slow relative to the time required to obtain the IR spectra.

Samples used in measurements of contact angles were removed from the reaction mixture, washed, dried briefly in air (5 min) and measured using sessile drop techniques described in detail elsewhere.[3] All contact angles were advancing angles. PE-CO$_2$H and its derivatives display a large hysteresis in contact angle, and retreating angles are often 0°. We have not established the origin of this pronounced hysteresis, but we suspect that it is due to swelling of the functionalized interface in contact with water. Despite the hysteresis, advancing contact angles are reproducible, and functional group concentrations inferred from them correlate well with estimates from independent techniques such as ATR-IR spectroscopy.[3,4] At pH 5, carboxylic acid groups present on the surface exist entirely in the protonated form (CO$_2$H); at pH 13, they are present entirely as the more hydrophilic carboxylate anion (CO$_2^-$). Contact angles measured at either value of pH are stable for periods of time much greater than 1 min (the time required to complete the measurement). Representative data are summarized in Figures 3 and 4.

For convenience in analysis, we have also represented data of the kind summarized in these figures in terms of the fractional progression, $\underline{f}$, of the parameter being measured from its initial to its final value (eq 1). Here $\underline{X}$ represents the measured property (IR or uv absorbance, cos θ_a, ESCA signal

$$\underline{f} = \frac{\underline{X}_t - \underline{X}_0}{\underline{X}_\infty - \underline{X}_0} \tag{1}$$

intensity) and $\underline{X}_\infty$ represents the asymptotic value of $\underline{X}$ at arbitrarily long reaction times. We choose, in order to make results from different types of
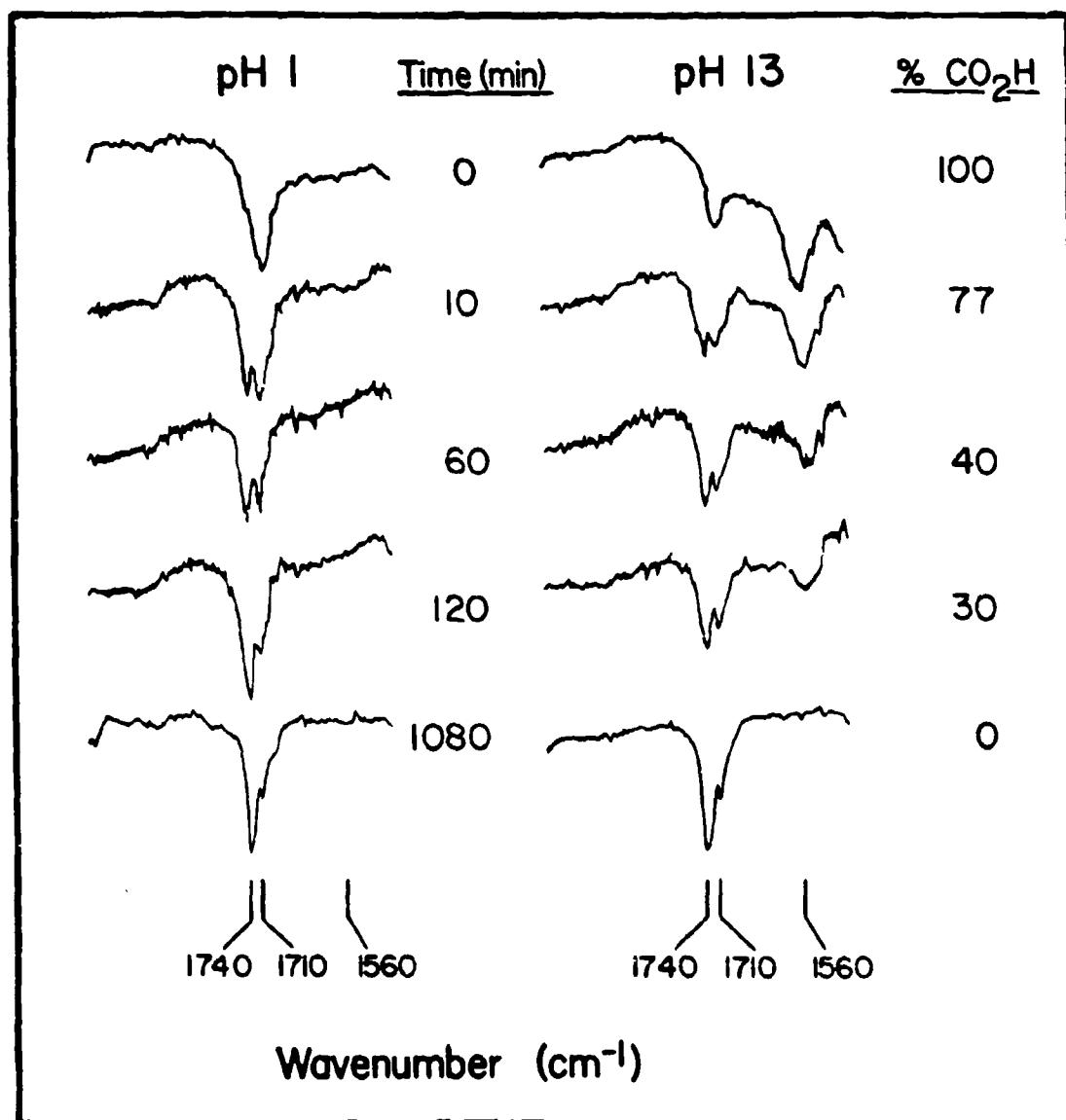
Figure 3. Representative ATR-IR spectra of PE-CO$_2$H taken after treatment of the film with acid (pH 1) or base (pH 13) obtained during acid-catalyzed esterification of the carboxylic acid groups in methanol. The absorption at 1560 cm^{-1} is due to the CO$_2^-$ group, and was the peak followed in determining the extent of reaction. The ester absorption occurs at 1740; the peak at 1710 includes both carboxylic acid and ketone groups.
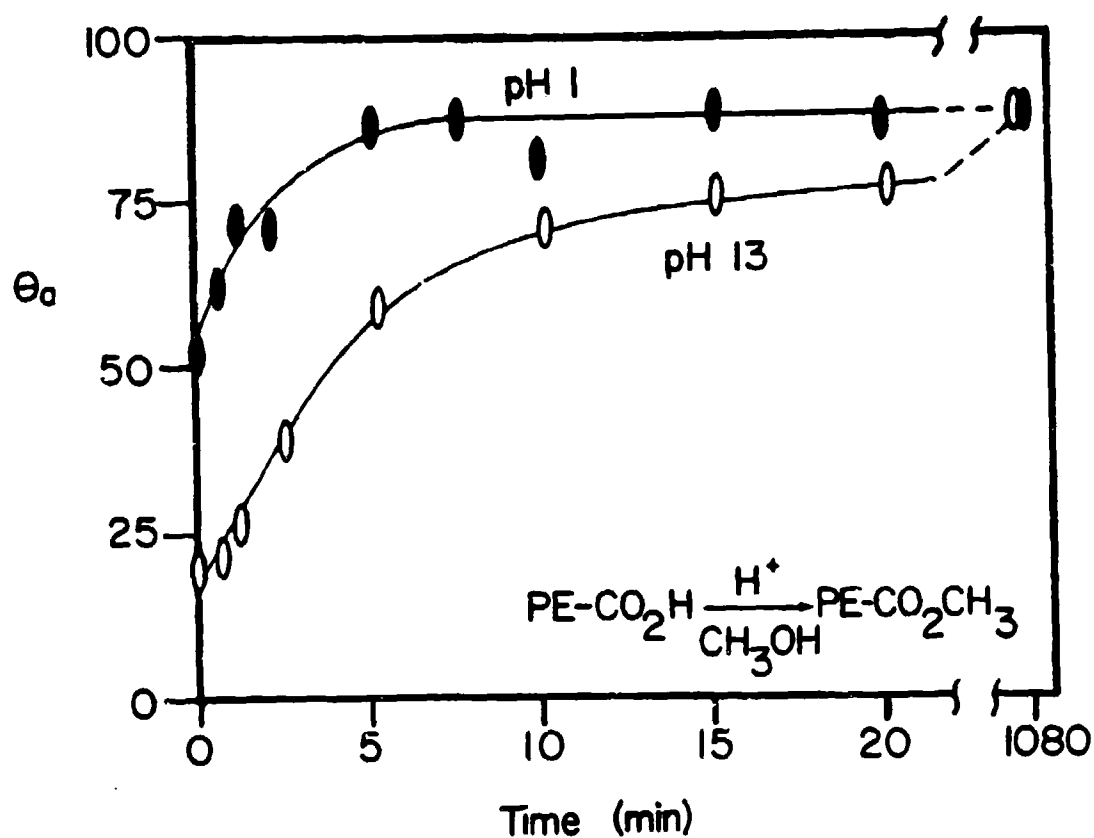
Figure 4. Representative contact angles observed during acid-catalyzed esterification of PE-CO₂H in methanol. Points were taken at pH 1 (0.1 N HCl) to observe CO₂H groups, and at pH 13 (0.1 N NaOH), to observe CO₂⁻ groups. Esterifications were conducted in anhydrous methanol containing 13% H₂SO₄ at 40 °C. The height of the symbols representing the data points are indicative of the estimated error bars in all figures except 5, 7, 8, 13 and 17.

experiments comparable, to have $\underline{f} = 0$ (at t = 0) and $\underline{f} = 1$ (at t = ∞). In order for $\underline{f}$ to describe the progression of a reaction, it is necessary that the properties symbolized by $\underline{X}$ be directly proportional to the extent of reaction. When $\underline{X}$ is a property such as uv absorbance, the relations between $\underline{X}$, the concentrations of chromophores, and the extent of reaction are well understood. For ESCA, the relationship is less obvious, because the sensitivity of this technique depends on the depth of the group being observed in the interface and on the nature of this group and the surrounding material. We have postulated that relationships of the type required by eq 1 hold for contact angle measurements and have presented experimental support for this postulate in the particular case of ionization of carboxylic acid groups.[3] This postulate must, however, still be considered unproved for a general case, and, in fact, data given in this paper suggest that it is only approximately correct even for carboxylic acids (see below).

In analyzing ATR-IR experiments, $\underline{X}$ was defined by eq 2 (A_{1560} indicates the absorbance at 1560 cm^{-1}). ATR-IR spectra were taken of samples

$$\underline{X}_{IR} = \frac{A_{1560}}{A_{1560} + A_{1740}} \qquad (2)$$

equilibrated, as indicated, at pH 13 to distinguish unesterified carboxylic acid moieties (as carboxylate ions with absorbance at 1560 cm^{-1}) from esters (1740 cm^{-1}) and ketones (1710 cm^{-1}). Figure 3 shows typical spectra.

The molecular-level interpretation of contact angles is complicated.[7-23] Contact angles are related to the relevant surface free energies using eq 3 (here, for example, γ_{SV} is the solid-vapor interfacial

$$\cos \theta = \frac{\gamma_{SV} - \gamma_{SL}}{\gamma_{LV}} \qquad (3)$$

free energy).[7] We assume, as we have previously,[3] that γ_{SV} and γ_{SL} are directly proportional to the relative populations of different surface species (eq 4a and 4b). In

$$\gamma_{LS} = \sum_j \beta_{j,LS} \gamma_{j,LS} \tag{4a}$$

$$\gamma_{SV} = \sum_j \beta_{j,SV} \gamma_{j,SV} \tag{4b}$$

$$\beta_{j,SV} \overset{?}{=} \beta_{j,LS} \tag{5}$$

equations 4 and 5, $\beta_{j,LS}$ is the normalized fraction of a particular type of organic group j in the population of groups in direct contact with the liquid phase (j = CO_2H, CO_2^-, CH_2, CH_3, CHO, C=O, and possibly others for $PE-CO_2H$) and $\gamma_{j,LS}$ ($\gamma_{j,SV}$) is the value of γ_{LS} (γ_{SV}) for a surface completely covered by the group j (β_j = 1). A usefully simple relation between X_θ and the physical observable cos θ <u>follows from the further assumption that $\beta_{j,SV} = \beta_{j,LS}$ (eq 5): that is, we assume that the composition and structure of the θ interphase is independent of the medium</u> (vapor, H_2O at pH 1, H_2O at pH 13) in contact with it. With this assumption, combination of eqs 3-5 yields eq 6. The extent of conversion f_θ can then be related to experimental values of contact angles by eq 7 (in both equations, experimental contact angles are advancing angles, although they are not so specified in the equations. Here, cos θ_0 is the initial value of cos θ, and cos θ_∞ is the final value: that is, respectively, the values at 0% and 100% reaction).

$$X_{\theta,t} = \cos \theta_t \tag{6}$$

$$f_\theta = \frac{\cos \theta_t - \cos \theta_0}{\cos \theta_\infty - \cos \theta_0} = \frac{\delta \cos \theta}{\Delta \cos \theta} \qquad (7)$$

The physical assumption underlying eq 5 is that the θ interphase is rigid, with a structure independent of its environment. This assumption is almost certainly incorrect in some and perhaps most experiments involving $PE\text{-}CO_2H$ and its derivatives in contact with water. One of the inferences to which the work in this paper leads is that the structure of this interphase does depend to some extent on its environment: that is, that it is sufficiently mobile (especially when in contact with water and partially swollen) to reconstruct--perhaps by allowing small motions of functional groups--in a manner that minimizes the interfacial free energy γ_{SL} (cf. the discussions below concerning the interpretation of Figures 17, 18 and 21). Although we do not believe eq 5 to be strictly correct, we assume it here in order to be able to derive equations 6 and 7 with simple forms. We find it more instructive and convenient to analyze the experimental data in terms of eq 7 and possible deviations from it--that is, in terms of possible failures of eq 5--than to try to carry through our discussions the intractable assumption of a solid-liquid interphase with variable composition and structure.

Contact angles can be measured using buffered aqueous drops having any chosen value of pH; we have routinely made parallel measurements of all samples at pH 1 (at which pH the CO_2H groups are fully protonated) and at pH 13 (where they exist as carboxylate anions, CO_2^-). These cases are distinguished by a subscript indicating the pH: e.g. $f_{\theta,pH\ 1}$ and $f_{\theta,pH\ 13}$.

Analyses of the extent of ionization α_1 (eq 8) of CO_2H groups in the θ interphase were carried out as described previously[3] by "contact angle titration": that is, measurement of contact angle of buffered aqueous solutions as a function of pH. The basis of this technique is the simplest

$$\alpha_1(pH) = \frac{[CO_2^-]}{[CO_2^-] + [CO_2H]} \tag{8}$$

$$\alpha_1(pH) = \frac{\gamma_{LS}(pH\ 1) - \gamma_{LS}(pH)}{\gamma_{LS}(pH\ 1) - \gamma_{LS}(pH\ 13)} \tag{9}$$

$$\alpha_1(pH) = \frac{\cos\theta_{pH} - \cos\theta_{pH\ 1}}{\cos\theta_{pH\ 13} - \cos\theta_{pH\ 1}} = \frac{\delta\cos\theta_a(pH)}{\Delta\cos\theta_a} \tag{10}$$

possible model of the polymer-water interface: that is, a model in which the only factor influencing the liquid-solid interfacial free energy is the interconversion of a constant population of surface CO_2H and CO_2^- groups. As indicated, data presented later in the paper bring the detailed correctness of this model into question. Despite a degree of uncertainty concerning the absolute accuracy of contact angle titration, it is clearly a useful technique for comparing θ interphases containing CO_2H groups. We discuss the limitations in our understanding of contact angle titration after summarizing the experimental data.
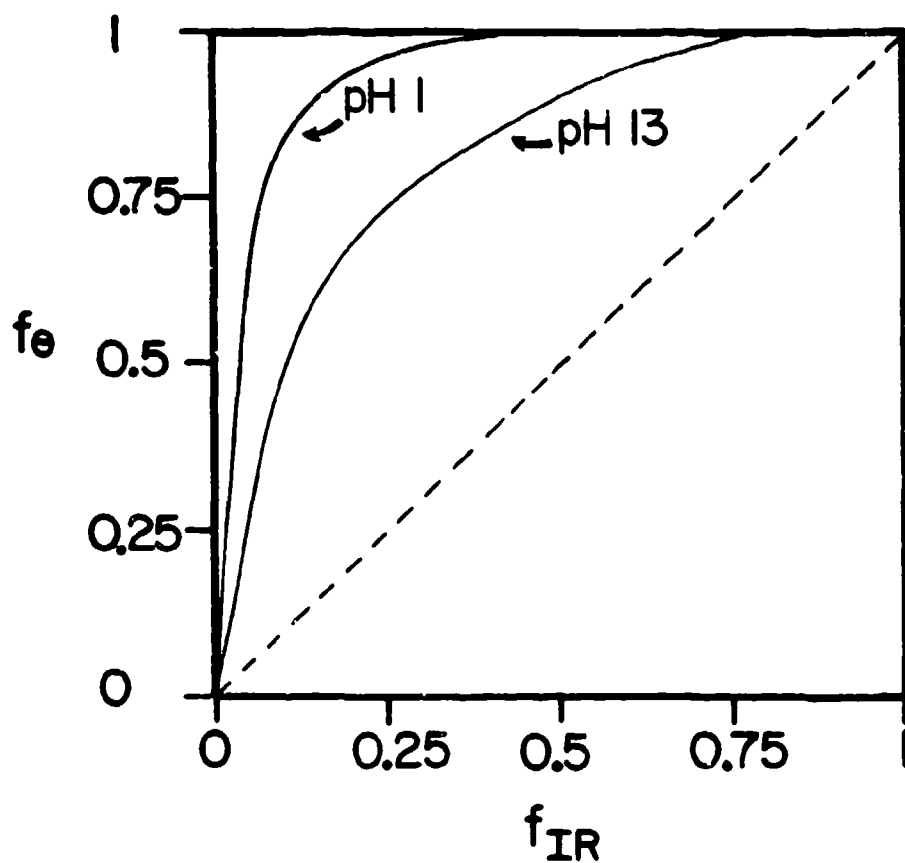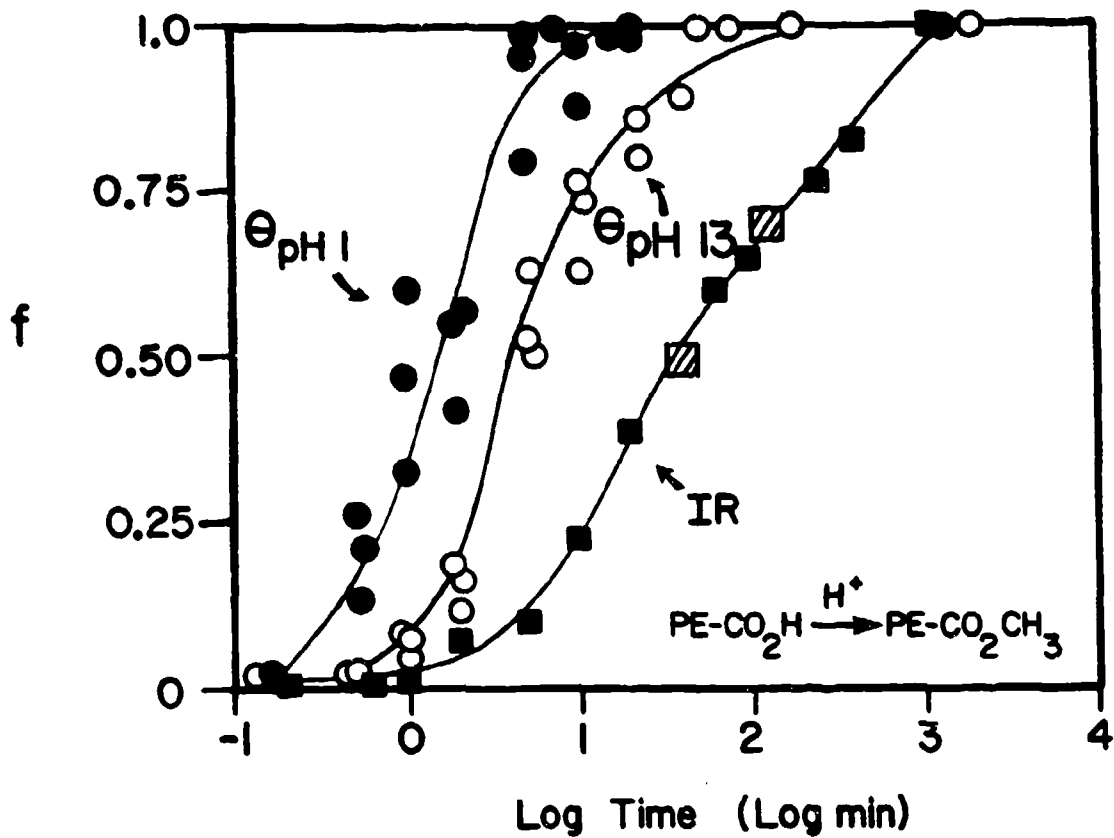
Results

Differential Esterification of the Carboxylic Groups of PE-CO$_2$H by Acid
Catalyzed Reaction with Methanol. PE-CO$_2$H[3] was suspended in anhydrous
methanol containing 13% v:v sulfuric acid at 40 °C, and the methanol was
stirred slowly. The conversion of CO$_2$H to CO$_2$CH$_3$ groups was followed by ATR-
IR spectroscopy and by contact angle (Figure 5). The use of a logarithmic
scale for time in this and similar plots carries no implication of underlying
processes with exponential form: it simply permits data collected for
processes having very different rates to be included in the same plot.

Figure 5 yields two important conclusions. First, the esterification
process(es) sensed by contact angle (both $f_{\theta,pH\ 1}$ and $f_{\theta,pH\ 13}$) proceed more
rapidly that that sensed by ATR-IR (f_{IR}). We infer that the carboxylic groups
in the θ interphase are those that react most rapidly, and that those present
deeper in the interphase region react more slowly. Second, $f_{\theta,pH\ 1}$ reaches
its limiting value more rapidly than $f_{\theta,pH\ 13}$. We suggest two possible
rationalizations for this difference, and note that data summarized later in
the paper favor the former: either the interphase containing hydrophilic
carboxylate groups can reconstruct (or at least, reconstruct more effectively
than an interphase containing only CO$_2$H groups) to present these hydrophilic
functionalities most effectively to the aqueous phase; or the contact angle
responds non-linearly to changes in the mole fraction of carboxylic acid
(carboxylate) groups present in the contact angle interphase.

The observation that chemical reactions in the θ interphase occur more
rapidly than those deeper in the functional interphase of PE-CO$_2$H implies that
it is possible to differentiate functional groups: one, a minority population
that influences contact angle and a second, majority population that is
detectable by ATR-IR but does not influence θ. To help in understanding the

Figure 5.   Top: Progression of contact angle ($f_{\theta,pH\ 1}$, $f_{\theta,pH\ 13}$; eq 7), and
ATR-IR (f_{IR}; eq 1 and 2) from initial to final values during acid-
catalyzed esterification of PE-CO$_2$H to PE-CO$_2$CH$_3$ (derived from the
data in Figures 3 and 4). The data points for $f_{\theta,pH\ 1}$ and
$f_{\theta,pH\ 13}$ are the result of three different experiments.
Similarly, the open squares contain the data points for three
different ATR-IR experiments. In this figure, and in figures 7,
8, 13 and 17, the errors associated with the experiment are best
estimated from the data scatter and thus the individual data
points are drawn smaller than their estimated error for clarity.
Bottom: The relationship between f_θ (pH 1 and pH 13) and f_{IR}
based on the data in the upper portion of the figure.

data in Figure 5, the lower portion of this figure gives plots of f_θ vs f_{IR}. This figure indicates that $f_{\theta,pH\ 1}$ has reached 0.9 before f_{IR} has reached 0.2. The difference for $f_{\theta,pH\ 13}$ is less extreme: $f_{\theta,pH\ 13} \simeq 0.9$ when $f_{IR} = 0.5$. Thus, esterification of <30% of the CO_2H groups detected by IR is sufficient to accomplish the full change in hydrophilicity of the surface detected by water at pH 1. Esterification of approximately 50% of the CO_2H groups detected by IR is required to complete the change in hydrophilicity detected at pH 13. We infer from these results that ~20-50% of the CO_2H groups in PE-CO_2H lie in the contact angle interphase.

The magnitude of this range and the difference between $f_{\theta,pH\ 1}$ and $f_{\theta,pH\ 13}$ are not surprising. The CO_2H groups in the θ interphase certainly have a degree of mobility. We hypothesize that the interfacial free energy is minimized at pH 13 by exposing the maximum possible number of CO_2^- groups; the thermodynamic driving force for exposing the less polar CO_2H group is smaller, and permits less surface reconstruction when the sample is brought into contact with water.

This model of the contact angle interphase as an entity whose structure depends in part on the extent and type of interaction between the functionalized polymer and the liquid in contact with its surface is a hypothesis that helps to rationalize the properties of the functionalized interface of PE-CO_2H. This hypothesis is consistent with data from several experiments (see below), but because of uncertainties in the microscopic interpretation of contact angles (Figure 1) it is not immediately helpful in defining the dimensions of the θ interphase. It is, for example, possible that the surface of PE-CO_2H is more swollen by water at pH 13 than at pH 1, and that this swelling (as opposed, for example, to reorientation of

carboxyl(ate) groups on a relatively rigid polyethylene layer) is responsible for the difference between $f_{\theta,pH\ 1}$ and $f_{\theta,pH\ 13}$.

Figure 5 contains one additional piece of information. The curve of f_{IR} vs time shows a significant break at $f_{IR} \simeq 0.5$. Although this break is suppressed by the logarithmic form of the time axis, the second half-life for the esterification processes followed by IR is ten times larger than the first. This observation indicates that the CO_2H groups present below the θ interphase esterify significantly more slowly than those in the θ interphase. We have surveyed the kinetics of the esterification reactions observed using changes in contact angle and ATR-IR. Figure 6 shows first-order kinetic plots for esterification based on f_{IR}, $f_{\theta,pH\ 1}$, and $f_{\theta,pH\ 13}$. For comparison, the figure includes data for the homogeneous esterification of acetic acid under these same conditions. Esterification of carboxylic acid moieties in the interphase of PE-CO_2H is much slower than esterification in solution. The half time in solution is $t_{1/2} \lesssim 0.1$ min. Carboxylic acid groups in PE-CO_2H esterify more slowly with $t_{1/2} \simeq 2$ min ($f_{\theta,pH\ 1}$), $t_{1/2} \simeq 5$ min ($f_{\theta,pH\ 13}$), and $t_{1/2} \simeq 45$ min (f_{IR}). We attribute the decreased rate of reaction on the polymer to exclusion of protons from the low dielectric constant region at the interface between the polymer ($\epsilon \gtrsim 2.3$) and the methanol ($\epsilon \bullet 33$) and perhaps to the low dielectric constant of the interfacial region itself. This exclusion would be more effective deeper in the interphase region. Both $f_{\theta,pH\ 1}$ and $f_{\theta,pH\ 13}$ appear to follow approximately first-order kinetics. This observation suggests that those groups in the θ interphase form a relatively homogeneous population with similar reactivity. In contrast, the progress of f_{IR} is clearly not first order: some CO_2H groups are much less reactive than others. We attribute the
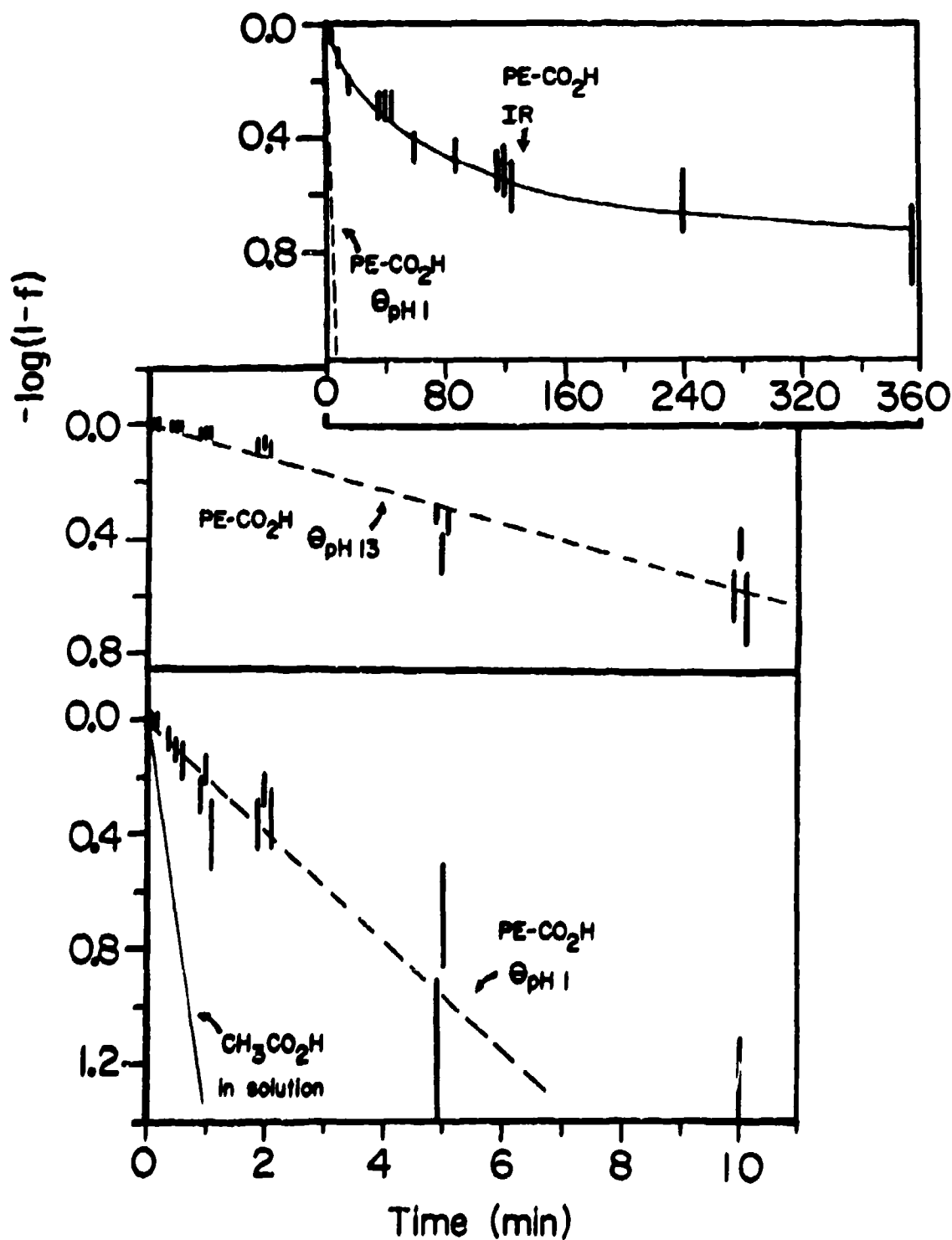
Figure 6. First-order kinetic plots for $f_{\theta,pH\ 1}$, $f_{\theta,pH\ 13}$ and f_{IR} for acid-catalyzed esterification. For comparison, the plot also includes data for the conversion of acetic acid to methyl acetate under the same conditions (followed by GC).

deviation from first-order behavior to a decrease in reactivity with depth in the interphase region.

Differential Hydrolysis of $PE-CO_2CH_3$. Extended treatment of $PE-CO_2H$ with methanol and acid results in complete esterification of the carboxylic acid groups present in the oxidatively functionalized interphase (as measured by ATR-IR). When the resulting material ($PE-CO_2CH_3$) is treated with either aqueous alkali or aqueous acid, these ester groups hydrolyze. Figure 7 summarizes values of f_θ and f_{IR} obtained by following the hydrolysis of the ester groups of $PE-CO_2CH_3$ in aqueous base; Figure 8 shows corresponding data for hydrolysis in aqueous acid.

Hydrolysis in aqueous base provides a clear distinction between reactivity in the θ interphase and reactivity deeper in the interphase (Figures 7 and 9). The contact angle in these experiments (both at pH 1 and pH 13) has reached its limiting value when only approximately one-third of the CO_2CH_3 groups observed by IR have hydrolyzed; at ∿50% (pH 1) and ∿70% (pH 13) conversion of the contact angle to its final value, only a 5-10% conversion of CO_2CH_3 to CO_2H (CO_2^-) groups has occurred by ATR-IR. As in the experiments involving differential esterification, it appears that ∿30% of the total carboxyl groups present in the sample occupy the θ interphase. The major contribution to the properties of the θ interphase may, however, come from 10% or less of the total population of carboxyl groups.

The kinetics of base-catalyzed hydrolysis (Figure 9) of $PE-CO_2CH_3$ appears to be first-order in the θ interphase ($f_{\theta,pH\ 1}$ and $f_{\theta,pH\ 13}$). This observation suggests again that the ester groups that constitute the θ interphase comprise a relatively homogeneous population. The kinetics are clearly not first-order for the total surface ester population: The plot of f_{IR} vs time shows a break after reaching $f_{IR} ≳ 0.3$ (Figures 7 and 9), and

Figure 7. Progression of f_θ and f_{IR} from initial to final values during base-catalyzed hydrolysis of $PE-CO_2CH_3$ in 1 N NaOH at T = 20 °C. The f_θ (pH 1 and pH 13) data points represent three different experiments. Similarly, the open squares represent three different ATR-IR experiments.

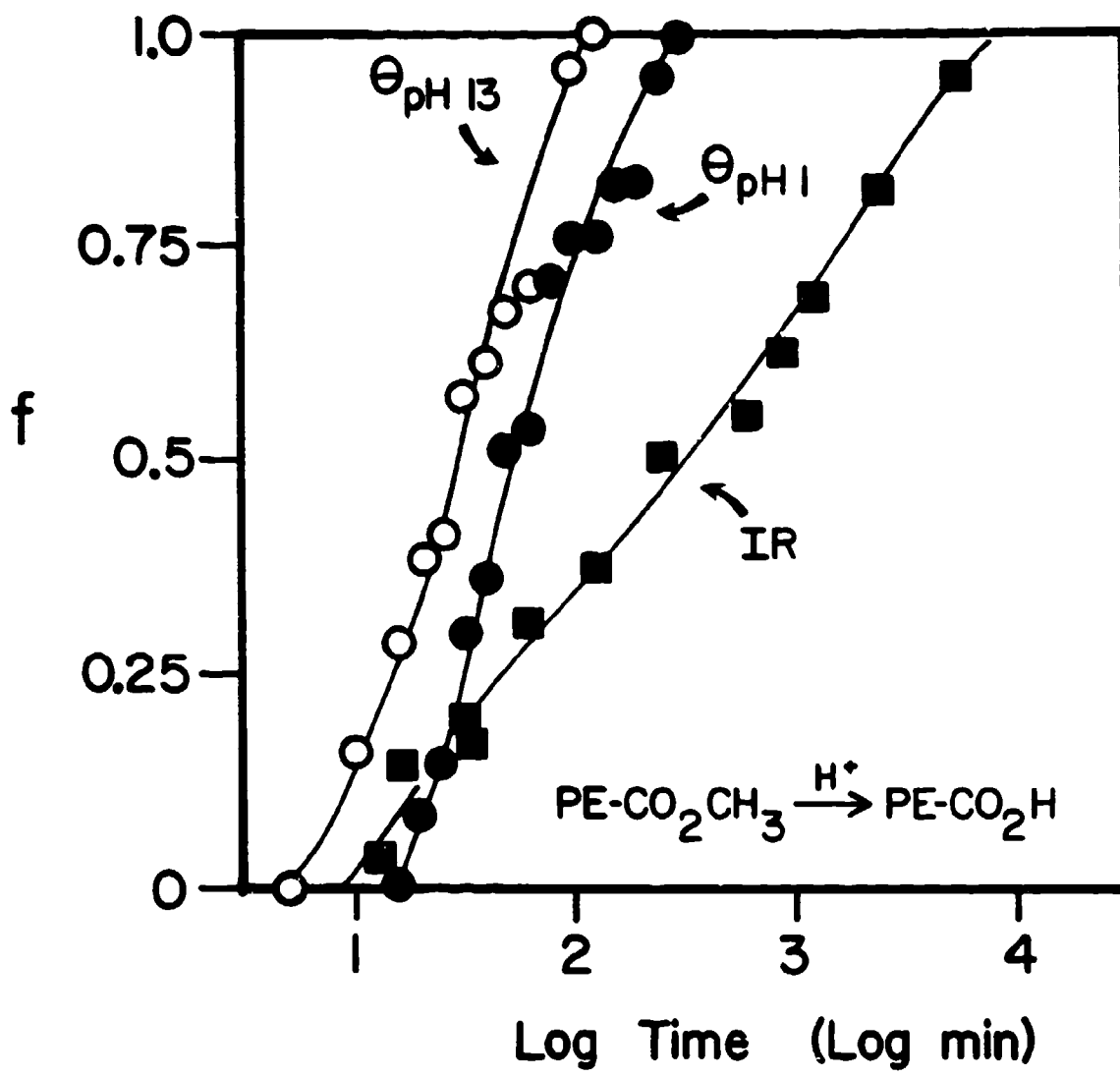Figure 8. Progression of f_θ and f_{IR} from initial to final values during acid-catalyzed hydrolysis of PE-CO$_2$CH$_3$ in 50% (w/w) H$_2$SO$_4$, T = 25 °C.
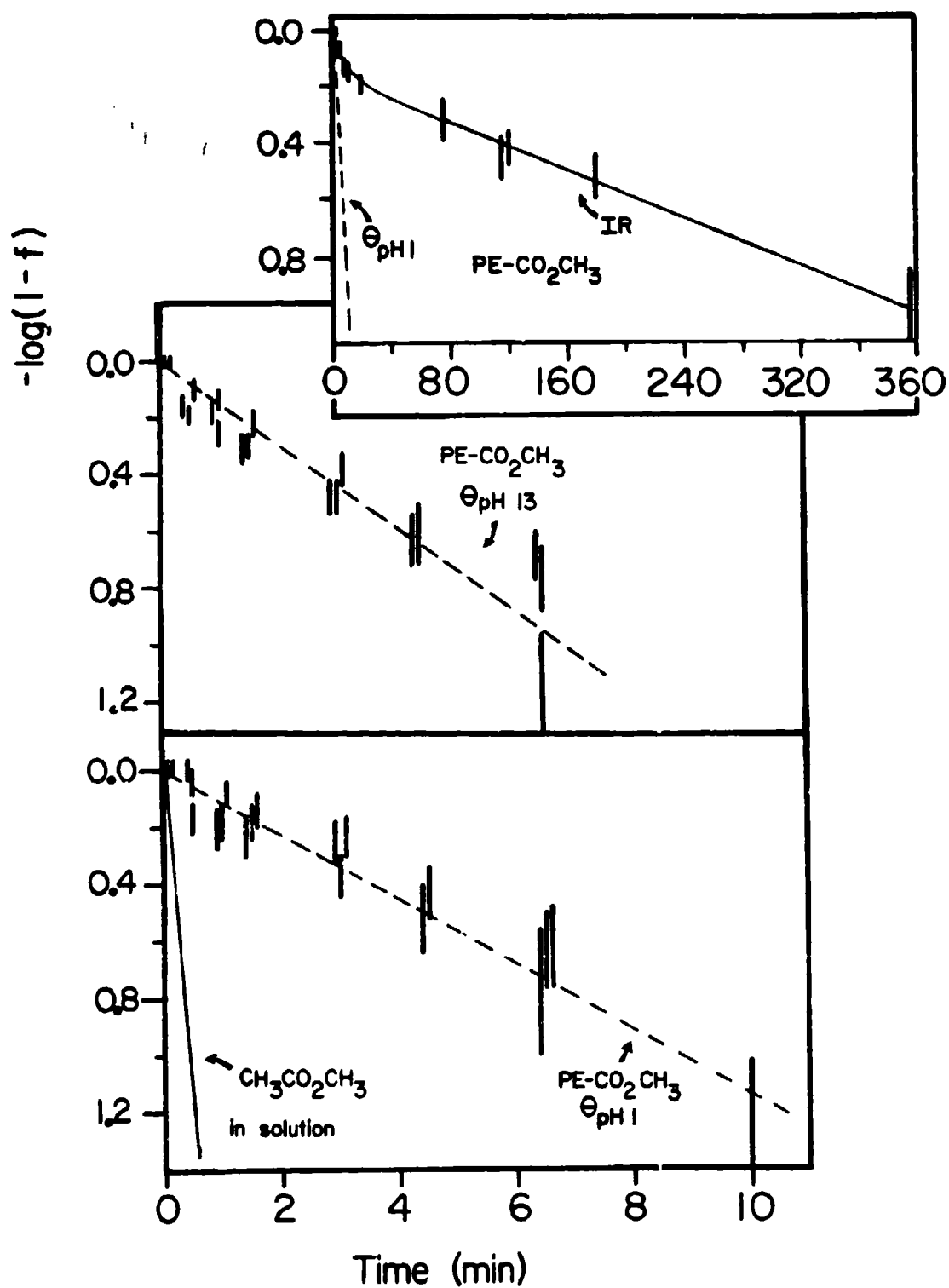
Figure 9.   First-order kinetic plots for $f_{\theta,pH\ 1}$, $f_{\theta,pH\ 13}$ and f_{IR} from the data of Figure 7. For comparison, the plot includes data for homogeneous hydrolysis of $CH_3CO_2CH_3$ under the same conditions.[25]

establishes that deeper esters are more difficult to hydrolyze than those in the θ interphase. The population of deeper (sub-θ interphase) esters may also consist of a uniformly-reacting population, since the kinetic plot for f_{IR} (Figure 9) can be fitted to two straight lines that intersect at $f \gtrsim 0.3$ (-log $(1 - f) \gtrsim 0.16$).

Base-catalyzed hydrolysis of the ester groups of $PE-CO_2CH_3$--both in the θ interphase (pH 1: $t_{1/2} \gtrsim 4$ min) and in the sub-θ interphase ($t_{1/2} \gtrsim 160$ min)--is much slower than the first-order hydrolysis of methyl acetate in aqueous solution at the same value of solution pH ($t_{1/2} = 0.13$ min).[25] We again attribute this decreased surface reactivity to some combination of effects leading to a decrease in the OH^- concentration in the surface region and to the lower dielectric constant in this region.

Acid-catalyzed hydrolysis (Figures 8 and 10) is similar to base-catalyzed hydrolysis, but less selective for the ester groups occupying the θ interphase: f_{IR} reaches ~ 0.5 before hydrolysis in the θ interphase is complete ($f_{\theta,pH\ 1} \sim 1$); in base-catalyzed hydrolysis, $f_{IR} \sim 0.3$ at this stage of hydrolysis. This difference is clearly important in efforts to develop synthetic methods that differentiate functional groups in the θ and sub-θ interphases and indicates that base-catalyzed hydrolysis provides the sharpest differentiation.

We have not established the mechanistic origin of the difference between acid- and base-catalyzed processes in detail. The θ and sub-θ interphases differ as media for hydrolysis reactions in several respects, of which polarity, viscosity, and ion-solvating ability are the most obvious. The rate of ester hydrolysis in homogeneous solution depends only slightly on polarity. The rate of base-catalyzed hydrolysis of methyl acetate decreases with decreasing polarity ($\underline{k} = 7.8$ M^{-1} min^{-1} in aqueous NaOH at 20 °C[25]; $\underline{k} = 5.1$ M^{-1} min^{-1} in 70% aqueous acetone containing NaOH at 20 °C[27]). Thus, the
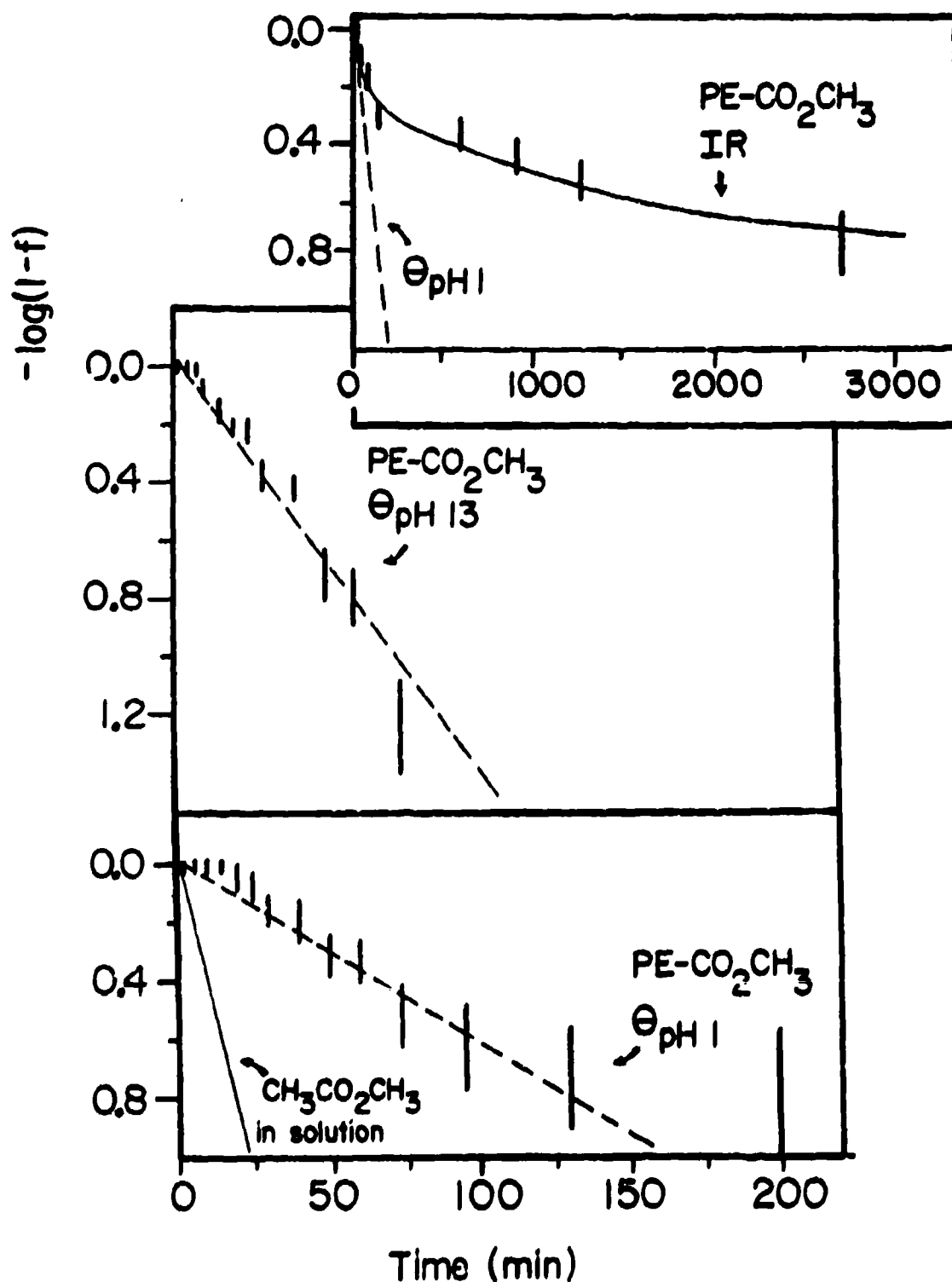
Figure 10. Kinetic plots for $f_{\theta, pH\ 1}$, $f_{\theta, pH\ 13}$ and f_{IR} from the data of Figure 8. For comparison, the plot includes data for homogeneous hydrolysis of $CH_3CO_2CH_3$ under the same conditions.[26]

polarity of the sub-θ interphase alone would result in a decreased reactivity in this region compared to the θ interphase. The expected magnitude of the decrease does not, however, seem large enough to rationalize the markedly decreased reaction rate in the sub-θ interphase. Hydrolysis rates also depend on the thermodynamic activity of water and acid and base catalysts; partitioning of hydronium and hydroxide into different regions of the interphase could well be different. Acid-catalyzed hydrolysis of ester groups generates CO_2H moieties; base-catalyzed hydrolysis generates the much more polar CO_2^- group. The polarity of the interphase (and thus the penetration of catalytic ions into the interphase) should change more markedly during base-catalyzed hydrolysis than during acid-catalyzed hydrolysis. All of these factors, and others, might contribute to the difference in selectivity of these reactions.

Reaction of PE-COCl with Water-Methanol Mixtures. Reaction of PE-CO$_2$H with PCl_5 converts all of the carboxylic acid groups present in the polymer to acid chloride functions.[3,4] Reaction of this material with water-methanol mixtures generates mixtures of carboxylic acid and methyl ester functionalities. Figure 11 gives plots analogous to those of Figures 5, 7, and 8 for reaction of PE-COCl and butyryl chloride with water-methanol mixtures in varying proportions. The vertical axis in this plot represents the fraction of COCl groups converted to ester rather than to acid moieties. In solution, this reaction is rapid and relatively unselective (Figure 11). The partitioning of acid chloride to methyl ester is approximately proportional to the mole fraction of methanol in the reacting solution. Although the reaction of PE-COCl also seems to be relatively non-selective, analysis based on ATR-IR suggests a higher selectivity for conversion to ester moities than in the homogeneous solution reaction at all concentrations of

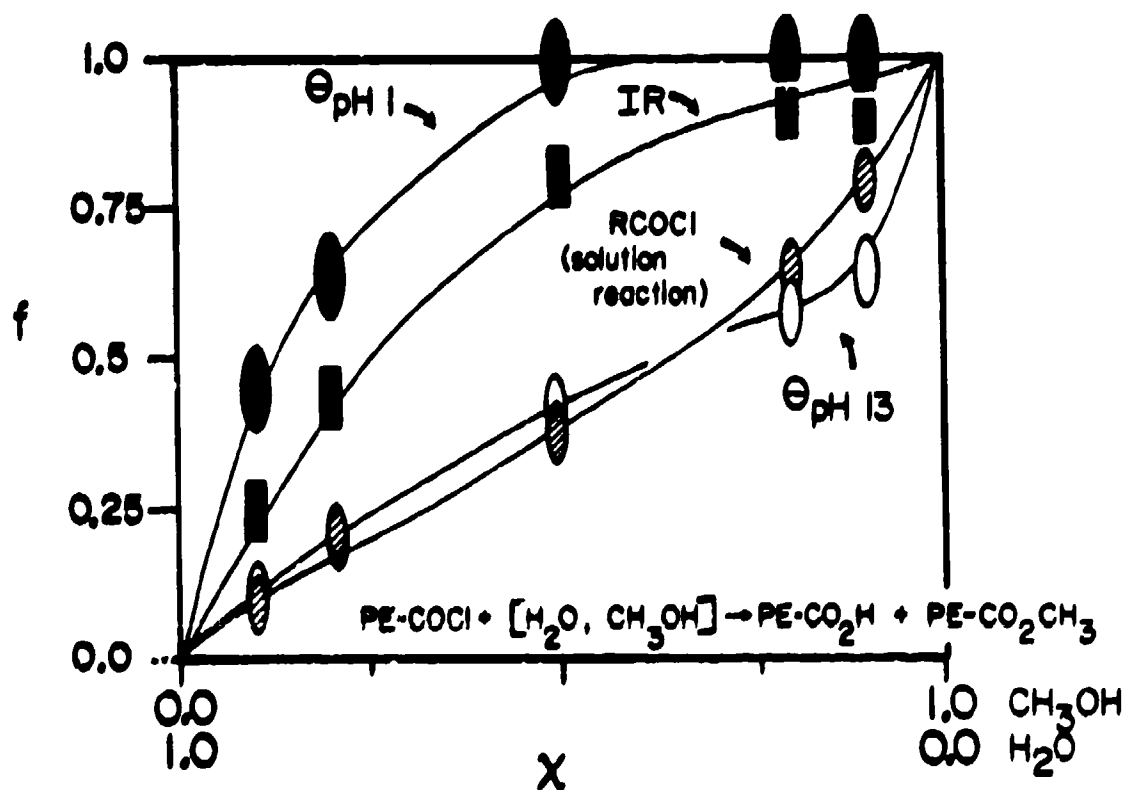Figure 11. Progression of f_θ (pH 1 and pH 13) and f_{IR} for reaction of PE-COCl
with water-methanol mixtures. The figure includes data for
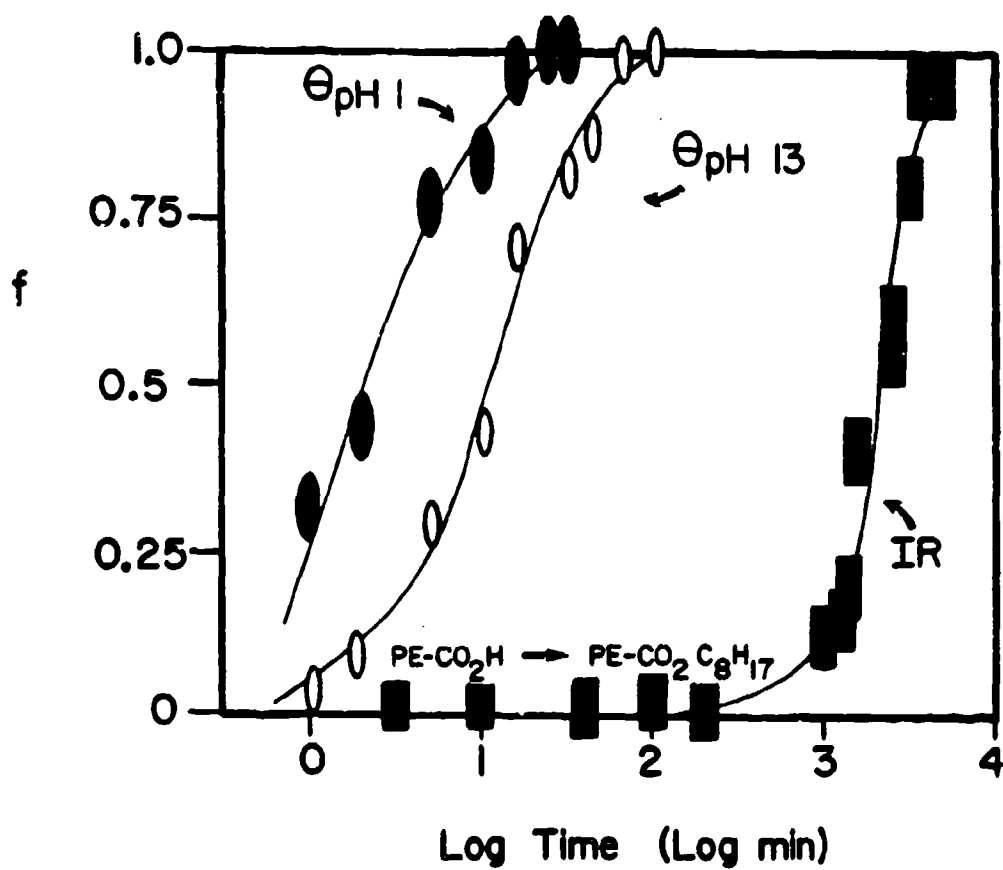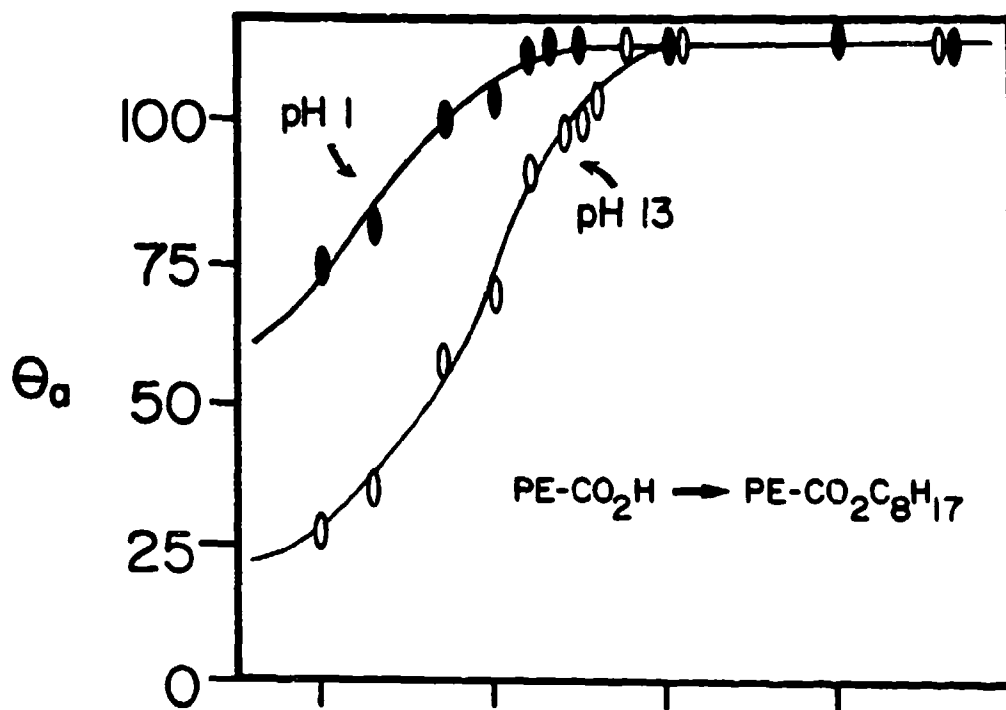butyric acid chloride under the same conditions (determined by
GC).

methanol. The difference between reactivities of PE-COCl and C_3H_7COCl might plausibly reflect preferential partitioning of methanol into the low-polarity functionalized polymer interface. More importantly, there is no evidence for different reactivity in the θ and sub-θ interphases: the total population of carbonyl groups ($CO_2CH_3 + CO_2H$) assayed by IR lies between the estimates from contact angle at pH 1 and pH 13.

The difference between estimates of partitioning between CO_2CH_3 and CO_2H based on measurements of contact angle are instructive. The data in Figure 11 are again compatible with the hypothesis that wettability in basic solution is disproportionately sensitive to CO_2^- groups. The rough agreement between IR analyses and analyses by contact angle at pH 1 suggests that the latter reasonably reflects concentrations of groups in the θ interphase, relatively unobscured by artifacts (surface swelling, rearrangement of positions of groups at the surface) that would maximize exposure of CO_2^- groups to the aqueous solution.

Differential Reactions Involving $PE-CO_2(CH_2)_7CH_3$. We have repeated the acid-catalyzed esterification and base-catalyzed hydrolysis--the reactions giving the sharpest discrimination between groups in the θ interphase and those deeper in the functionalized interphase--using the n-octyl ester of $PE-CO_2H$, $PE-CO_2C_8H_{17}$, as product or reactant (Figures 12 and 13). Differentiation of the reactivity of groups present in the θ interphase appears to be markedly different in these processes than in the corresponding reactions involving $PE-CO_2CH_3$.

The acid catalyzed esterification (Figure 12) follows the same general trends as for $PE-CO_2CH_3$ except that the extent of reaction by IR (f_{IR}) is negligible (<0.05) when reaction is complete by contact angle ($f_{\theta,pH\ 1} = 1$). We attribute the conversion of the polymer surface to a hydrophobic form, at

Figure 12. <u>Top</u>: Progression of $\theta_{pH\ 1}$ and $\theta_{pH\ 13}$ for the acid-catalyzed esterification of PE-CO$_2$H in octanol (300 mL) containing H$_2$SO$_4$ (75 mL) at 40 °C. <u>Bottom</u>: Progression of $f_{\theta,pH1}$, $f_{\theta,pH13}$ and f_{IR} for the acid-catalyzed esterification of PE-CO$_2$H. The values for f_θ were determined from the data in the upper portion of the figure by using equation 7.

Top panel axis labels: Θ_a (vertical), values 0, 25, 50, 75, 100.
Labels: pH 1, pH 13, $PE\text{-}CO_2H \longrightarrow PE\text{-}CO_2C_8H_{17}$

Bottom panel axis labels: f (vertical), values 0, 0.25, 0.5, 0.75, 1.0.
Labels: $\Theta_{pH\,1}$, $\Theta_{pH\,13}$, IR, $PE\text{-}CO_2H \longrightarrow PE\text{-}CO_2C_8H_{17}$

Horizontal axis: Log Time (Log min), values 0, 1, 2, 3, 4.
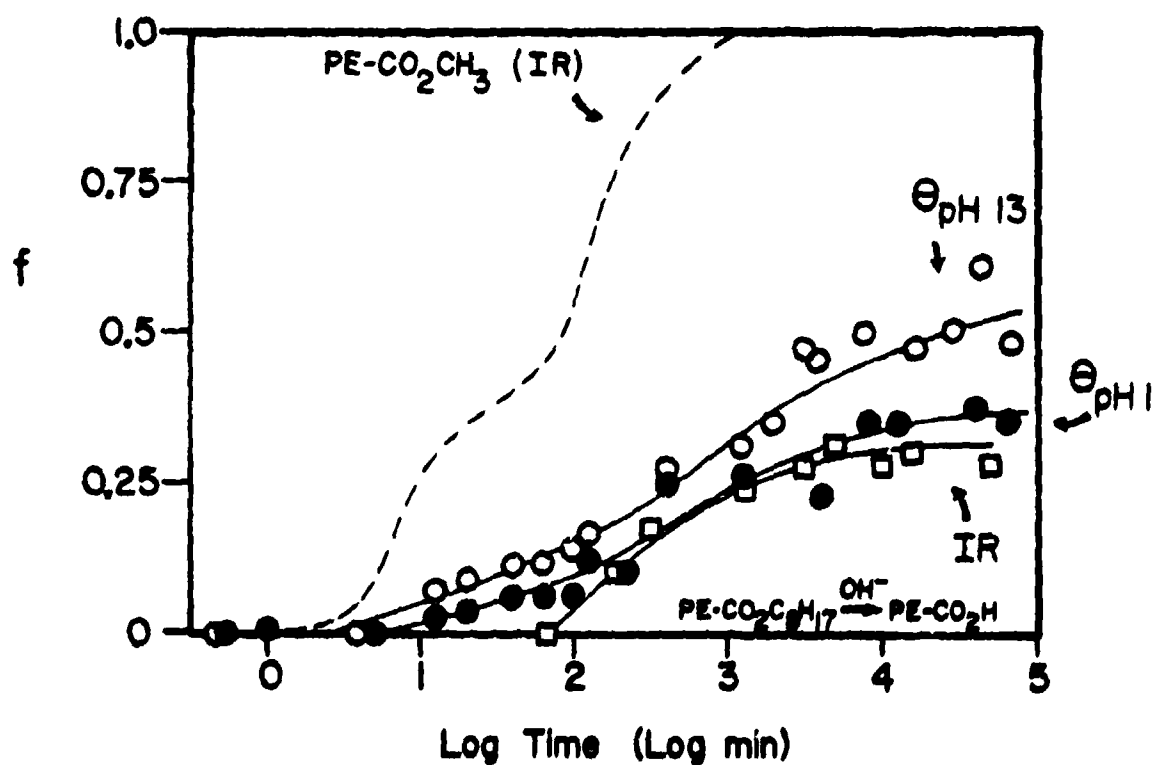
Figure 13. Progression of $f_{\theta,pH\ 1}$, $f_{\theta,pH\ 13}$, and f_{IR} for the base-catalyzed hydrolysis of $PE-CO_2C_8H_{17}$ in 1 N NaOH at 20 °C. The curve for the base-catalyzed hydrolysis of $PE-CO_2CH_3$ determined by IR (Figure 7) is shown for comparison.

very low total conversion of acid to ester groups, to the ability of the long, hydrophobic octyl moieties to cover the surface (Figure 14A) much more effectively than methyl groups (Figure 14B). Thus, when ~10% of the acid groups in the θ interphase (that is, 10% of 30% or ~3% of the total acid groups in the polymer) have been esterified with octyl groups the surface appears, from the vantage of the contacting aqueous phase, to be composed entirely of hydrocarbon chains. At the same conversion of acid to ester groups, the methyl ester surface still has many CO_2H groups in contact with the liquid phase. We note that the limiting contact angles for $PE-CO_2C_8H_{17}$ with water ($\theta_{pH\ 1} = 125°$; $\theta_{pH\ 13} = 125°$) are significantly higher than for $PE-CO_2CH_3$ ($\theta_{pH\ 1} = 90°$; $\theta_{pH\ 13} = 90°$) and in fact higher than for unfunctionalized polyethylene itself ($\theta_{pH\ 1} = 103°$; $\theta_{pH\ 13} = 103°$). The esterification in the sub-θ interphase (f_{IR}) by $\underline{n}$-octyl alcohol proceeds more slowly than esterification by methanol by a factor of 10 to 100.

Base-catalyzed hydrolysis of $PE-CO_2C_8H_{17}$ also differs significantly from that of $PE-CO_2CH_3$ (Figures 13, 15). The hydrolysis of $PE-CO_2C_8H_{17}$ is not only >1000 times slower than that of $PE-CO_2CH_3$ under similar conditions but also follows a different kinetic course. While base-catalyzed hydrolysis of esters in the θ interphase of $PE-CO_2CH_3$ was kinetically first-order (by $f_{\theta,pH\ 1}$ and $f_{\theta,pH\ 13}$) but non-first order by f_{IR}, $PE-CO_2C_8H_{17}$ does not follow first-order kinetics in any of these parameters. Further, values of f_{IR}, $f_{\theta,pH\ 1}$ and $f_{\theta,pH\ 13}$ are not significantly different at any time during the reaction. We attribute both of these differences to a major difference in the compositions and structures of the θ and sub-θ interphases of $PE-CO_2C_8H_{17}$ and $PE-CO_2CH_3$. The ester moieties of $PE-CO_2C_8H_{17}$ are surrounded by octyl groups, some of which originate in esters lying in the sub-θ interphase of the polymer (Figure 14C), and it is necessary to hydrolyze a large fraction of the total
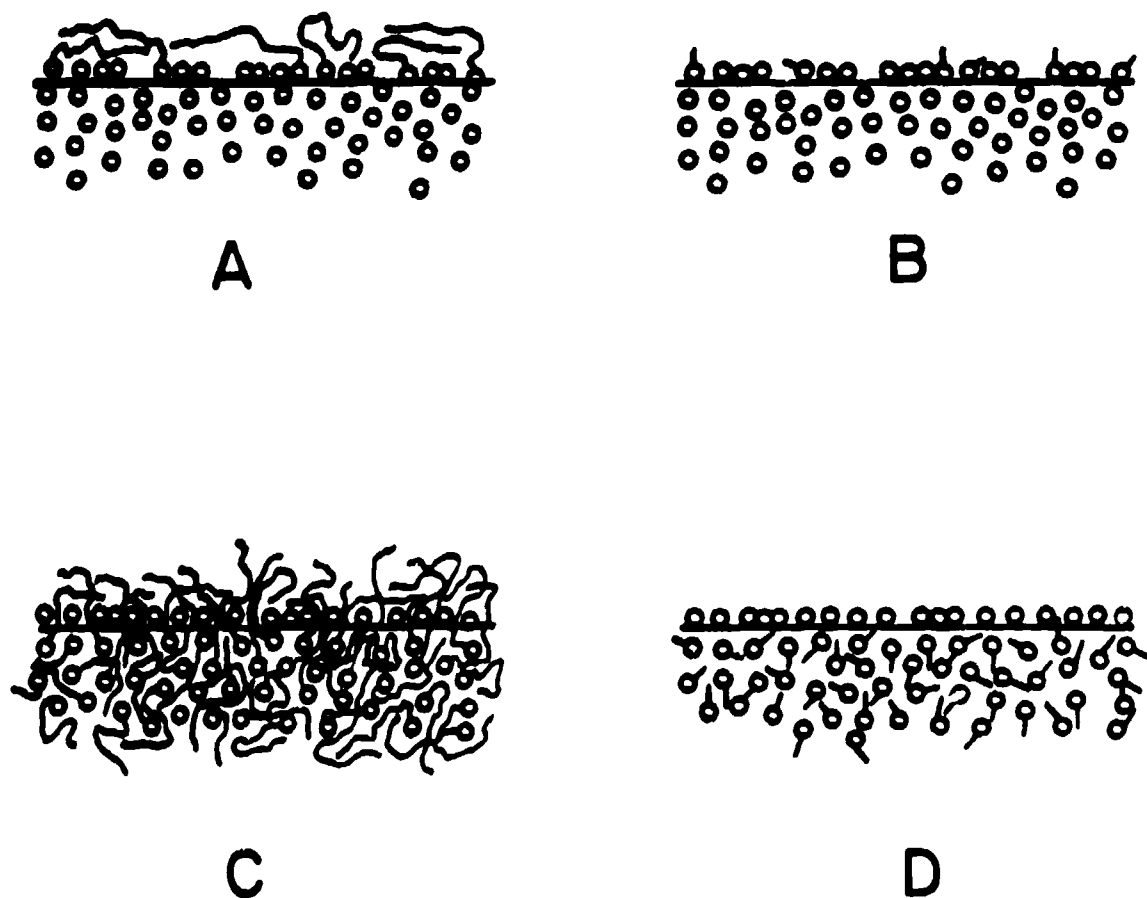
Figure 14. Schematic illustrations of: A) a partially esterified PE-CO₂H surface using octanol; B) a partially esterified PE-CO₂H surface using methanol; C) a partially hydrolyzed PE-CO₂C₈H₁₇ surface; D) a partially hydrolyzed PE-CO₂CH₃ surface.
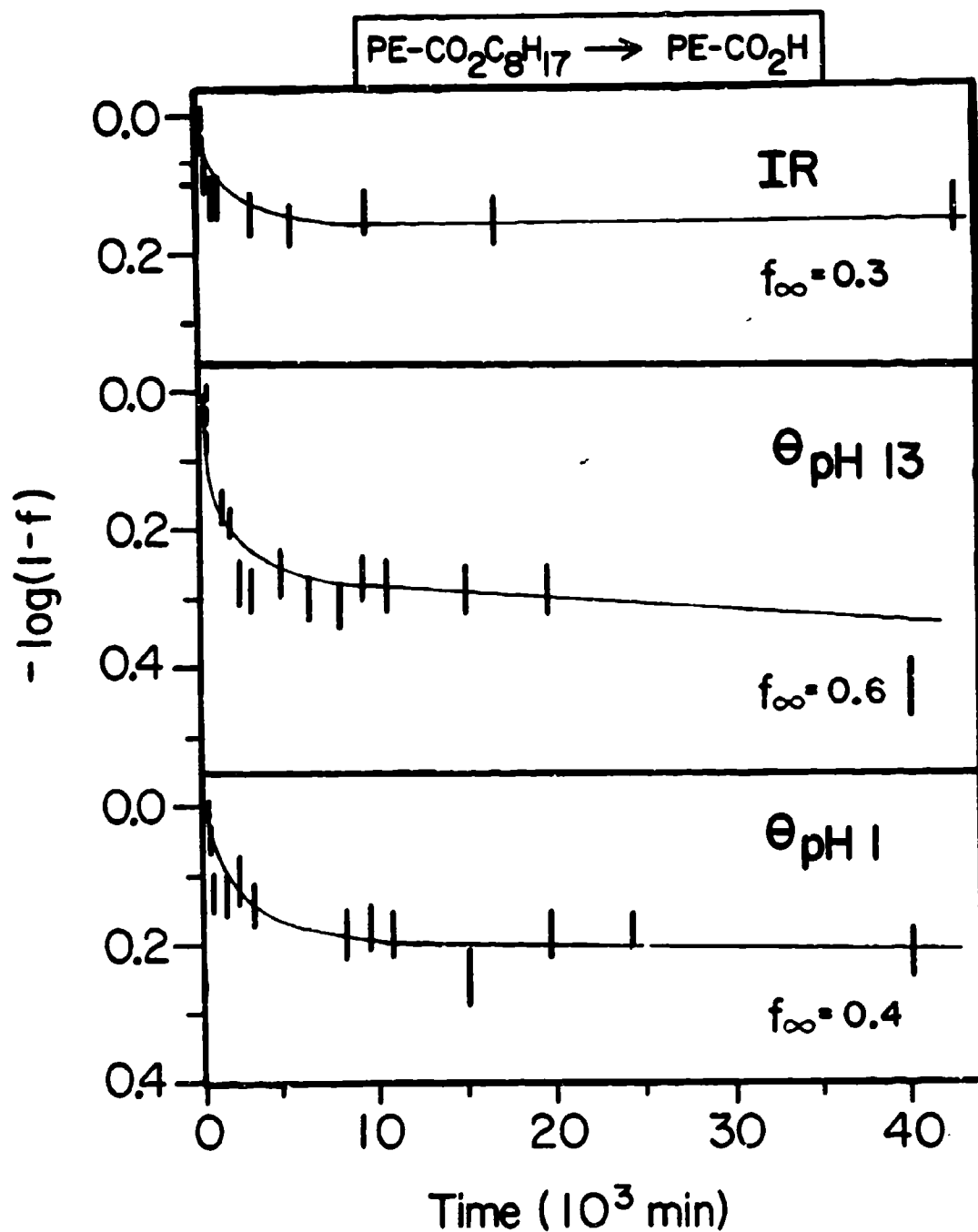
Figure 15. First-order kinetic plots for f_θ and f_{IR} for the base-catalyzed hydrolysis of PE-$CO_2C_8H_{17}$ using the data in Figure 13. The values of f reached after ~3 weeks in base (30,000 min) are indicated on the figure. Beyond this point, little reaction takes place up to >80,000 min.

ester groups present before the θ interphase becomes as hydrophilic as the material generated on hydrolysis of PE-CO_2CH_3 surface and near-surface ester groups (Figure 14D).

We have attempted to test this structural hypothesis by examining the hydrolysis of a sample of PE $\overline{CO_2H}CO_2C_8H_{17}$ in which the ester groups are the minimum required to cover the surface (Figure 14A). PE-CO_2H was esterified with acid in octyl alcohol just long enough to complete the reaction occurring in the θ interphase (Figure 13, 100 min). The surface of this material was then exposed to base and hydrolyzed (Figure 16). Hydrolysis of this partially esterified surface proceeds to completion ($f_θ = 1$) much faster than does that of completely esterified PE-$CO_2C_8H_{17}$ (although still much more slowly than that of PE-CO_2CH_3). Thus, in samples in which it is unnecessary to hydrolyze esters lying below the θ interphase, hydrolysis proceeds smoothly to completion.

Hydrolysis of PE-CO_2R. A series of esters (PE-CO_2R, R = methyl to octyl), were prepared by acid-catalyzed esterification and exposed to base (1 N NaOH) and the hydrolysis of each was followed by contact angle. Table I lists the time to reach $f_{θ,pH\ 1} \simeq 0.5$ for each sample. It is clear that as the ester length increases, the $t_{1/2}$ increases dramatically. Such an increase is not observed in a structurally analogous set of acetate esters in aqueous solution. The rate of hydrolysis of these compounds is essentially the same for n-butyl, n-propyl, and ethyl esters, and these are only slightly less reactive than the methyl ester.

This difficulty in hydrolyzing the longer PE-CO_2R esters probably reflects the two considerations mentioned previously: the hydroxide ions must partition into an interphase that is thicker and has lower dielectric constant for the longer-chain esters than for the shorter chain ones, and a larger
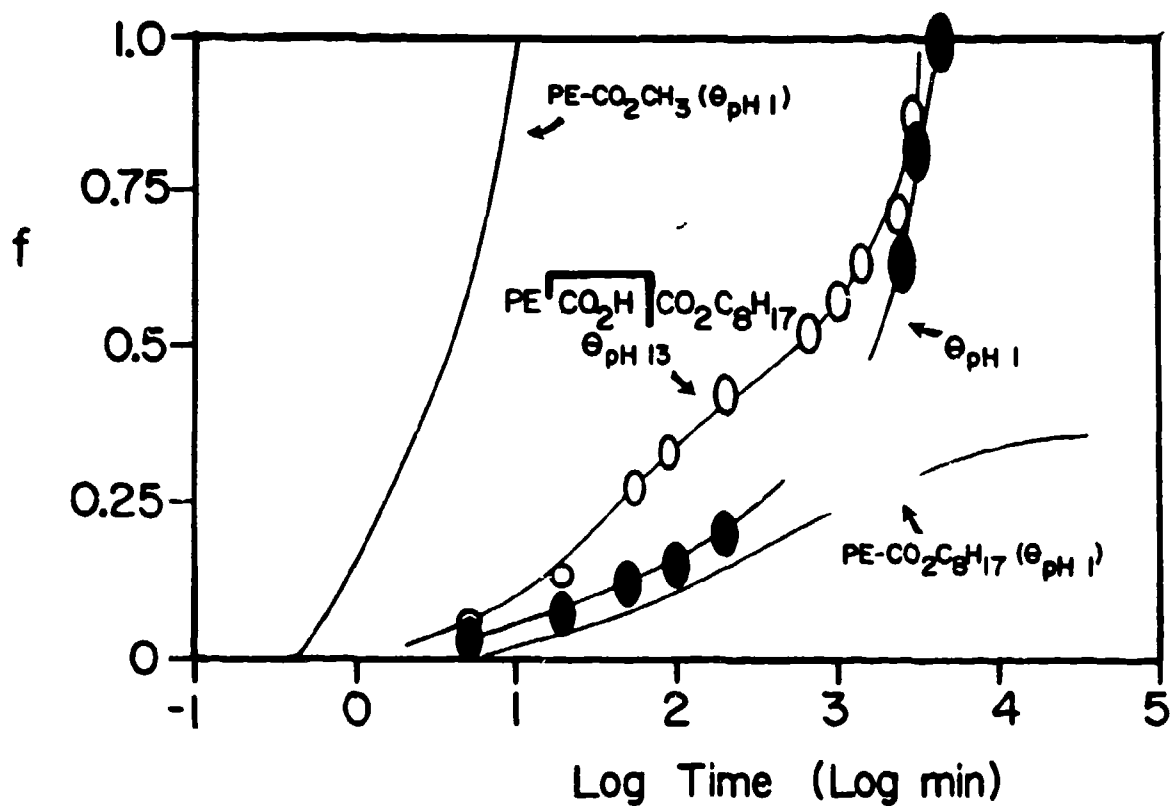
Figure 16. Progression of $f_{\theta,pH\ 1}$ and $f_{\theta,pH\ 13}$ for a partially esterified sample of PE-CO$_2$H using octanol (Figure 13, log t = 2.0), similar to that shown in Figure 14. The curves of $f_{\theta,pH\ 1}$ for PE-CO$_2$CH$_3$ and PE-CO$_2$C$_8$H$_{17}$ are shown for comparison.

Table I. Rates of base-catalyzed (1 N NaOH) hydrolysis of PE-CO$_2$R and CH$_3$CO$_2$R.

Ester	θ_i[a]	θ_f[b]	PE-CO$_2$R $t_{1/2}$[c]	PE-CO$_2$R k/k_{meth}[d]	CH$_3$CO$_2$R[e] $t_{1/2}$[c]	CH$_3$CO$_2$R[e] k/k_{meth}[d]
methyl	90	54	4.0	1	0.13	1
ethyl	103	56	20	0.2	0.22	0.6
n-propyl	106	55	800	0.005	0.24	0.5
i-propyl	110	57	800	0.005	0.79	0.2
n-butyl	116	nr	7250	0.0006	0.25	0.5
s-butyl	115	nr	6250	0.0006	1.22	0.1
n-hexyl	123	nr	>40,000	<0.0001	--	--
n-octyl	125	nr	>80,000	<0.00005	--	--

a θ_i is the contact angle (pH 1) on the surface before hydrolysis.

b θ_f is the contact angle after completion of hydrolysis. nr indicates that this point was never reached.

c $t_{1/2}$ (min) is the time to reach the midpoint of the reaction using eq 5.

d k/k_{meth} is the ratio of the rate constant of the particular ester divided by the rate constant of the methyl ester.

e From reference 25.

fraction of the total esters present must be hydrolyzed to achieve a given hydrophilicity.

Contact Angle Titration Curves (θ_a vs pH) for Surfaces Containing Mixtures of Esters and Acids. We have demonstrated that CO_2H and CO_2R groups present in the θ interphase can be differentiated from those deeper in the polymer by taking advantage of differences in reactivity in these different regions of the interphase. The preparative techniques outlined in previous sections permit the fraction x_{CO_2H} (eq 11) of the carboxylic acid groups in the mixture of carboxylic acid and carboxylic ester groups on the surface to be varied from 0 to 1.

$$x_{CO_2H} = \frac{[CO_2H]}{[CO_2H] + [CO_2CH_3]} \qquad (11)$$

We have determined full titration curves--θ_a as a function of pH for buffered aqueous solutions--using samples with different values of x_{CO_2H} prepared using acid-catalyzed esterification of PE-CO_2H in methanol, base-catalyzed hydrolysis of PE-CO_2CH_3, and reaction of PE-COCl with H_2O/CH_3OH mixtures. The objective of these studies is to understand the influence of the environment provided by the functionalized interphase of derivatives of PE-CO_2H on the ionization of CO_2H groups in the θ interphase. We are specifically interested in three questions: Is the acidity of these groups influenced by their density in the θ interphase? How does their acidity respond to changes in the polarity of the θ interphase? Does the character of the sub-θ interphase influence the acidity of CO_2H groups present in the θ interphase?

Figure 17 (bottom) summarizes data obtained at different extents of conversion of CO_2H to CO_2CH_3 groups by acid-catalyzed esterification. For convenience, the plots also indicate approximate values of bulk solution pH at which initial ionization occurs ($\alpha_i = 0$; α_i, the extent of ionization, is defined by eq 8); and at which ionization is complete ($\alpha_i = 1$); $pK_{1/2}$ is the value of solution pH at which we estimate $\alpha_i \sim 0.5$. These parameters refer only to carboxylic acid moieties in the θ interphase.

The most striking feature of these data is the difference in the response at low and high values of pH. The wettability of these three types of surfaces reaches its limiting value at pH 5 significantly before it does so at pH 11. We attribute this difference, as indicated, to a disproportionately larger influence of CO_2^- than CO_2H on wettability at low concentrations and/or to different structures for the θ interphase in acidic and basic media.

In more detailed terms, the shifts in the pH at which $\alpha_i = 0$ and in the $pK_{1/2}$ suggest that the acidity of the CO_2H groups in the θ interphase becomes less as neighboring CO_2H groups in the θ-interphase are esterified. These data do not, by themselves, distinguish between a shift in acidity due to changes in surface polarity and one due to selective esterification of more acidic groups in a heterogeneous population.

Data from pH-θ_a titration for base-catalyzed hydrolysis of PE-CO_2CH_3 (Figure 17, top) and for non-depth selective conversion of PE-COCl to a mixture of carboxylic acid and methyl ester groups (Figure 17, middle) show qualitatively similar trends. This observation argues against selective esterification and hydrolysis as the origin of the shift of, e.g. $pK_{1/2}$ to larger values as x_{CO_2H} decreases, since it is unlikely that these three types of reaction would result in selective exposure of the same set of CO_2H groups. Thus, we propose that the origin of this shift in acidity is a change

Figure 17. <u>Upper</u>: Plots of θ_a vs pH for esterification of PE-CO$_2$H. The plot on the right gives the fraction of total carboxyl groups present as carboxylic acids (x_{CO_2H}, eq 11, derived from f_{IR}). The dotted lines in the plots give the values taken as $\alpha_i = 0$, $\alpha_i = 0.5$ ($p\underline{K}_{1/2}$) and $\alpha_i = 1.0$. <u>Middle</u>: Plots of θ_a vs pH for surfaces made by reacting PE-COCl with CH$_3$OH/H$_2$O mixtures. <u>Bottom</u>: Plots of θ_a vs pH for base-catalyzed hydrolysis of PE-CO$_2$CH$_3$.
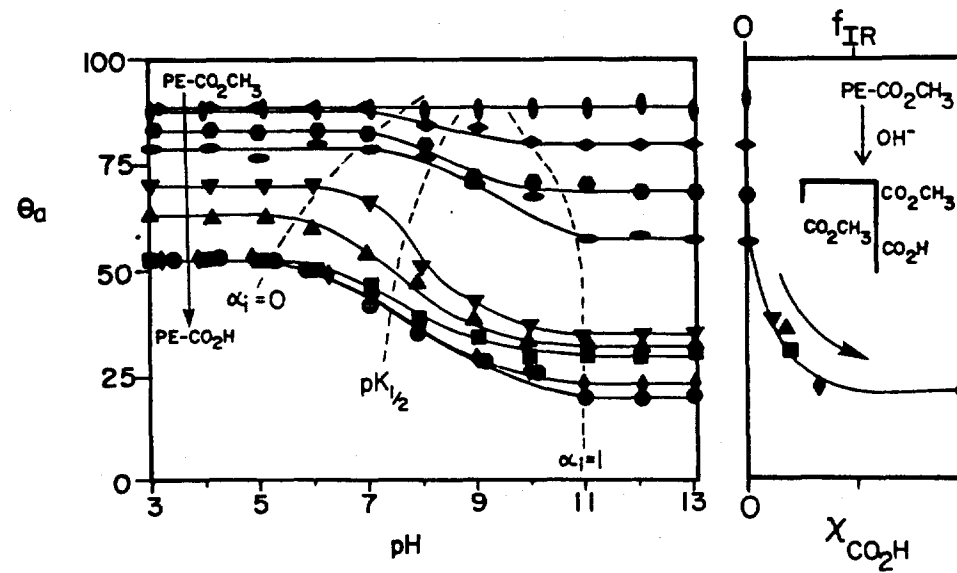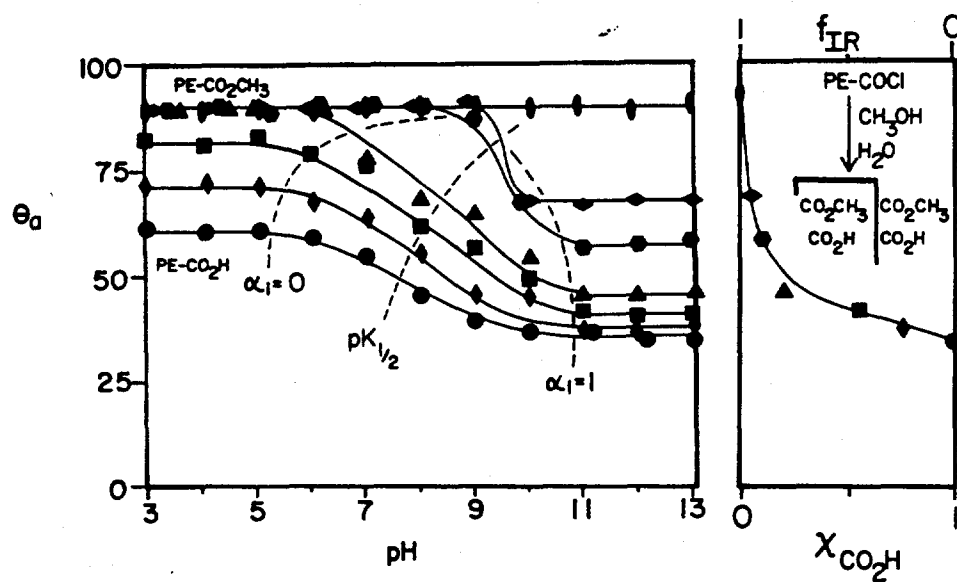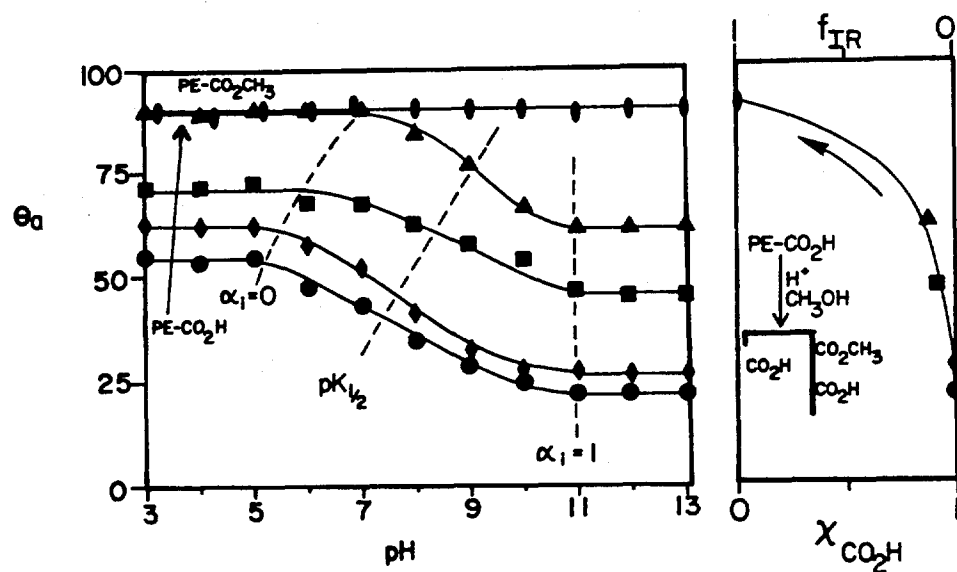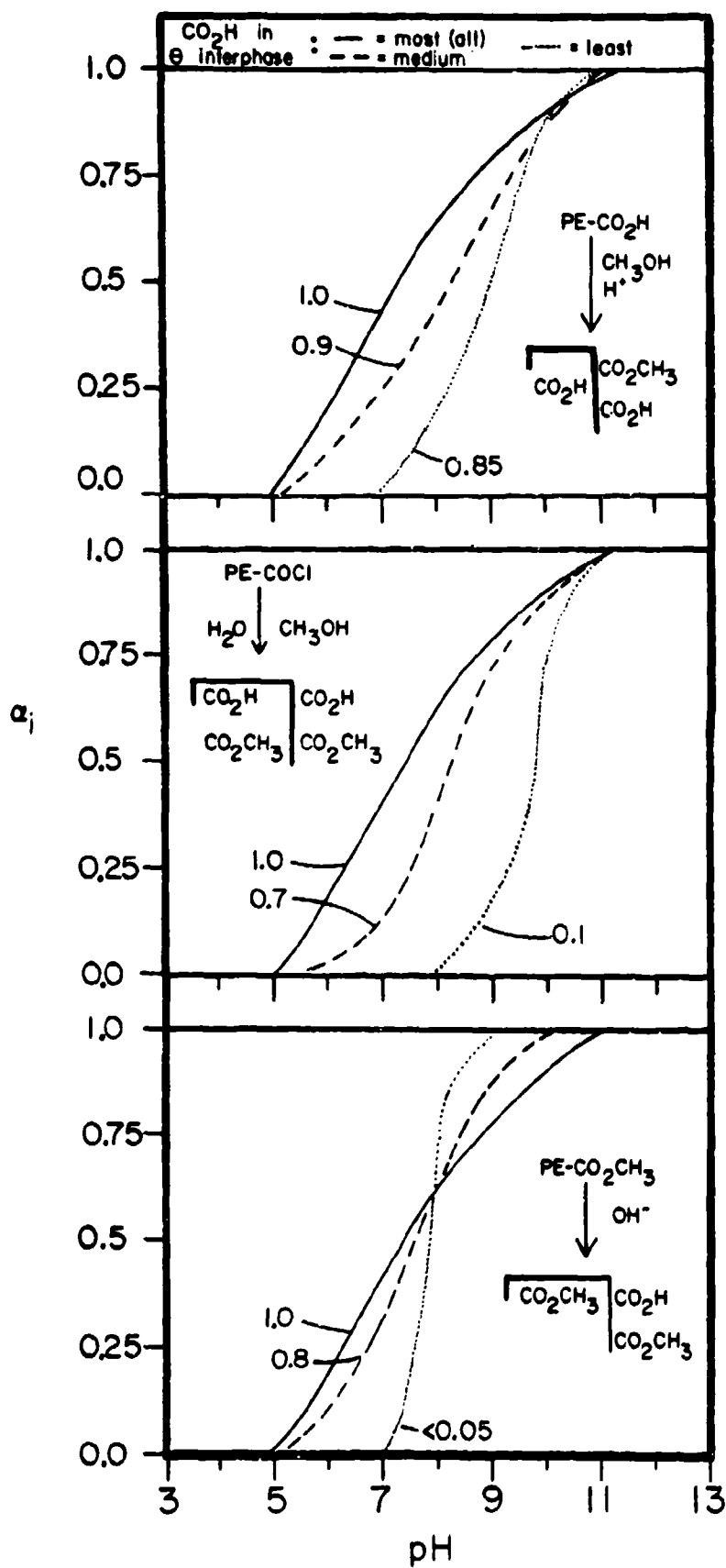
in polarity of the θ interphase. As a larger fraction of the CO_2H groups in this interphase are converted to esters, the interphase becomes less polar and ionization of the remaining CO_2H groups more difficult. Similar shifts are well-documented both in small molecules[28], in proteins,[29] and in solutions of differing polarity.[30-32]

We examine the ionization of the surface CO_2H groups in greater detail in Figure 18 by plotting representative curves of α_i vs pH for different values of x_{CO_2H}. Several features of these graphs are interesting. First, in each experiment, as x_{CO_2H} decreases, the width of the ionization curve decreases and the initial ionization point ($\alpha_i \gtrsim 0$) shifts to higher pH values. The decrease in the width of the curve probably reflects a decrease in charge-charge repulsion between carboxylate ions in the interfacial region. The shift to a higher pK_a ($\alpha_i = 0$) is presumably due to decreased polarity in the interfacial region. Second, the sub-θ interphase groups appear to influence the ionization of groups in the θ interphase. We do not believe that this influence on the groups in the θ interphase arises from differences in the polarity of the sub-θ interphase for three reasons. First, the average concentration of functional groups in the sub-θ interphase is not, in all probability, very high. A number of functional groups comparable to those in the θ interphase are distributed in the sub-θ interphase over a thicker layer and a larger volume. The average polarity of the sub-θ interphase may thus not be much influenced by interconversion of CO_2CH_3 and CO_2H groups. Second, CO_2H and CO_2CH_3 groups are not, in fact, very different in polarity.[33] Third, it is not clear how a change in polarity in the sub-θ interphase could influence ionization of θ-interphase groups, even if the change in polarity were large.

Figure 18. <u>Upper</u>: Plots of the extent of ionization α_i of the CO_2H groups

present on the surface of PE $\overline{CO_2H}|CO_2CH_3$ at different extents of

esterification of PE-CO_2H. The curves were determined from the

data in Figure 17 using eq 10. The numbers attached to the lines

represent the fraction of the mixture of CO_2H and CO_2CH_3 groups

present as CO_2H (x_{CO_2H}, eq 11). Continuous lines represent

surfaces with only CO_2H groups in the θ interphase ($\theta_{pH\ 1} \gtrsim 55°$).

Dashed lines represent surfaces with roughly equal numbers of

methyl ester and acid groups in the θ interphase ($\theta_{pH\ 1} \gtrsim 73°$).

Dotted lines represent those samples with just enough carboxylic

acid groups in the θ interphase to obtain an accurate contact

angle titration ($\theta_{pH} = 90°$; ester/acid ~ 5 in θ interphase).

<u>Middle</u>: Same as upper portion for surfaces made by reaction of

PE-COCl with water/methanol mixtures. <u>Bottom</u>: Same as upper

portion for surfaces made by base-catalyzed hydrolysis of

PE-CO_2CH_3.

Legend (top panel):
CO$_2$H in — most (all) ·········· least
⊖ interphase – – – medium

Panel 1 (top): curves labeled 1.0, 0.9, 0.85
Reaction scheme:
PE-CO$_2$H
CH$_3$OH
H$^+$
CO$_2$H CO$_2$CH$_3$
        CO$_2$H

Panel 2 (middle): curves labeled 1.0, 0.7, 0.1
Reaction scheme:
PE-COCl
H$_2$O   CH$_3$OH
CO$_2$H   CO$_2$H
CO$_2$CH$_3$ CO$_2$CH$_3$

Panel 3 (bottom): curves labeled 1.0, 0.8, <0.05
Reaction scheme:
PE-CO$_2$CH$_3$
OH$^-$
CO$_2$CH$_3$ CO$_2$H
             CO$_2$CH$_3$

Y-axis: α_i (0.0, 0.25, 0.5, 0.75, 1.0)
X-axis: pH (3, 5, 7, 9, 11, 13)

Our interpretation of the influence of sub-θ interphase groups on the ionization of θ-interphase groups is based on coulombic interactions. Charge-charge interactions act over relatively long ranges (tens of angstroms)[34] and could thus permit charged carboxylate anions in the sub-θ interphase to influence the ionization behavior of carboxylic acid species in the θ interphase. The result of these coulombic interactions would be to broaden the ionization range of the acid moieties in the θ interphase, as in soluble polybasic acids.[35] This hypothesis is consistent with the experimental data in Figure 18. For example, surfaces with low carboxylic acid concentrations in the θ-interphase (where charge-charge interactions between θ-interphase groups are at a minimum, shown as dotted lines in Figure 18) show curves that are much broader when carboxylic acids comprise the sub-θ interphase (Figure 18, top; 4 pH units) than when a mixture of esters and acids (Figure 18, middle, 3 pH units) or only esters (Figure 18, bottom; 2 pH units) are present in the sub-θ interphase. (We emphasize, however, that the experimental and analytical uncertainties involved in generating the curves in Figure 18 from the measurements of contact angles are significant, and small differences between these curves may not be significant.)

Ionization of Carboxylic Acid Groups Lying below the Contact Angle Interphase. PE-CO$_2$H that has been partially esterified with octanol (Figure 13, log t/min = 3.2) shows only saturated aliphatic groups in the θ interphase (θ_a = 125° at pH 5 or pH 13). These esters constitute, however, only ~20% of the total carboxylic acid/ester moieties detected in the functionalized interphase by ATR-IR. Although the remaining 80% of carboxylic acid groups do not influence the contact angle, they are, nonetheless, titratable using aqueous base.[36] The ability to convert carboxylic acid groups in the θ

interphase selectively to esters offers the opportunity to examine the acid/base behavior of the remaining, deeper carboxylic acid groups.

We have described the procedure used to determine the relation between α_i and pH for PE-CO_2H by ATR-IR spectroscopy previously in detail.[3] Ionization is defined, as previously, by eq 12 and 13 where A_{1560} is the absorbance at 1560 cm^{-1} (CO_2^-),

$$R_{(pH)} = \frac{A_{1560} \ (pH)}{A_{1560} \ (pH) \ + \ A_{1710} \ (pH)} \tag{12}$$

$$\alpha_i = \frac{R_{pH \ 1} \ - \ R_{(pH)}}{R_{pH \ 1} \ - \ R_{pH \ 14}} \tag{13}$$

A_{1710} is the overlapping absorbance at 1710 cm^{-1} (C=O, CO_2H) and at 1740 cm^{-1} (CO_2R). The sample is assumed to be fully protonated at pH 1 and fully deprotonated at pH 14. Figure 19 shows the quality of representative ATR-IR data. Figure 20 compares curves of α_i as a function of solution pH obtained for PE-CO_2H and the partially esterified film. The shape of the ionization curves are similar, with the esterified sample being ~2 pH units less acidic.

This result is consistent with previous conclusions regarding the factors influencing the ionization of carboxylic acid groups in the different interphases of PE-CO_2H. Charge-charge interactions should be similar in PE$\overline{CO_2H}CO_2C_8H_{17}$ and in PE$\overline{CO_2H}CO_2$H since only ~20% of the total groups present in the latter have been esterified in the former. The width of the ionization curve should therefore be similar for the two materials. The local polarity under a packing of octyl chains would, however, be expected to be quite low. This low polarity would shift the ionization curve to more basic values of solution pH, as is observed.
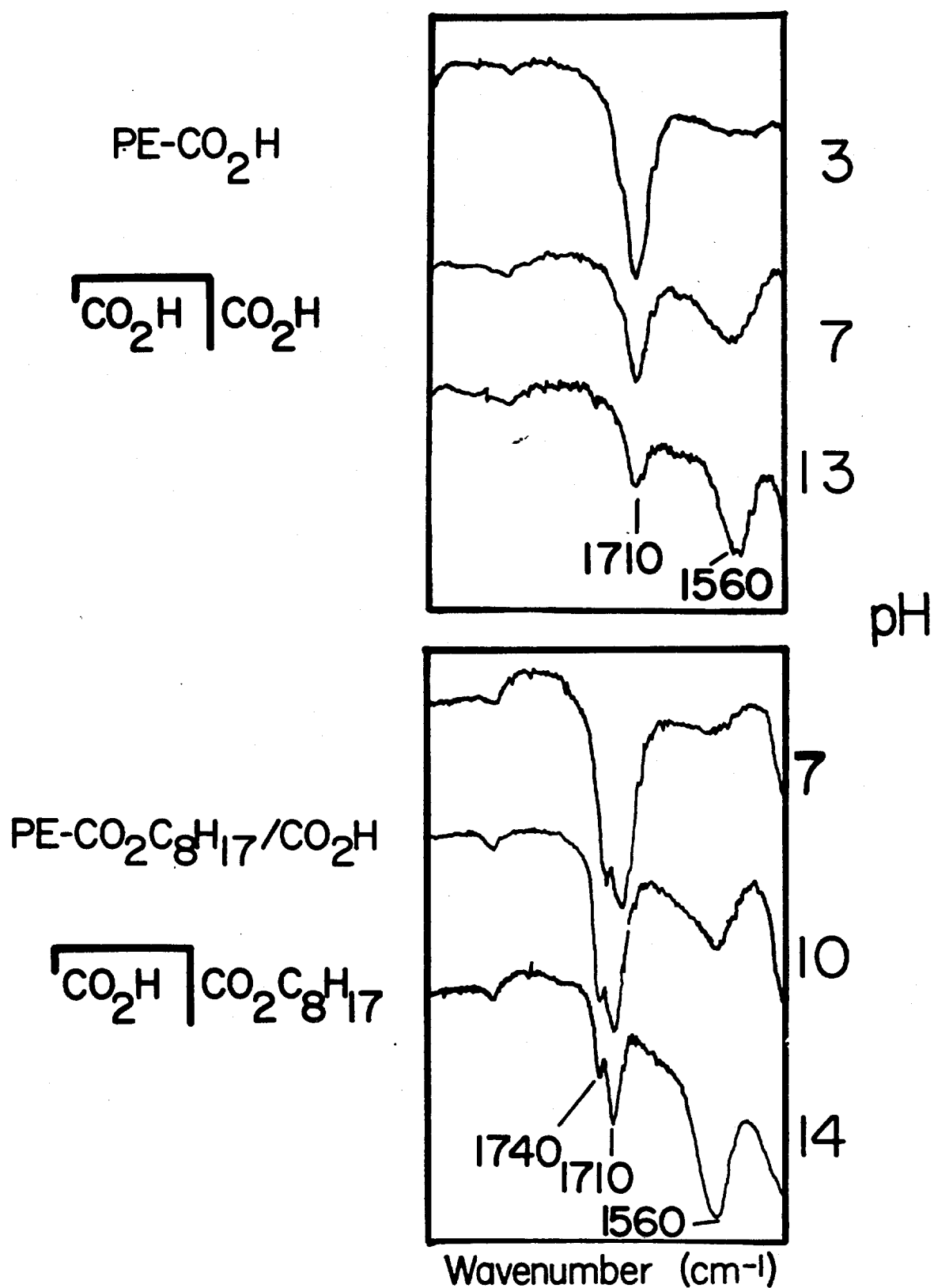
PE-CO$_2$H

$\lceil$CO$_2$H$\rceil$CO$_2$H

PE-CO$_2$C$_8$H$_{17}$/CO$_2$H

$\lceil$CO$_2$H$\rceil$CO$_2$C$_8$H$_{17}$

3

7

13

pH

7

10

14

1710

1560

1740 1710

1560

Wavenumber (cm^{-1})

Figure 19. Types of curves used in ATR-IR determinations of α_i vs pH for PE-CO$_2$H and the sub-θ interphase of partially esterified PE-CO$_2$H using octanol (Figure 12, lot t = 3.2).
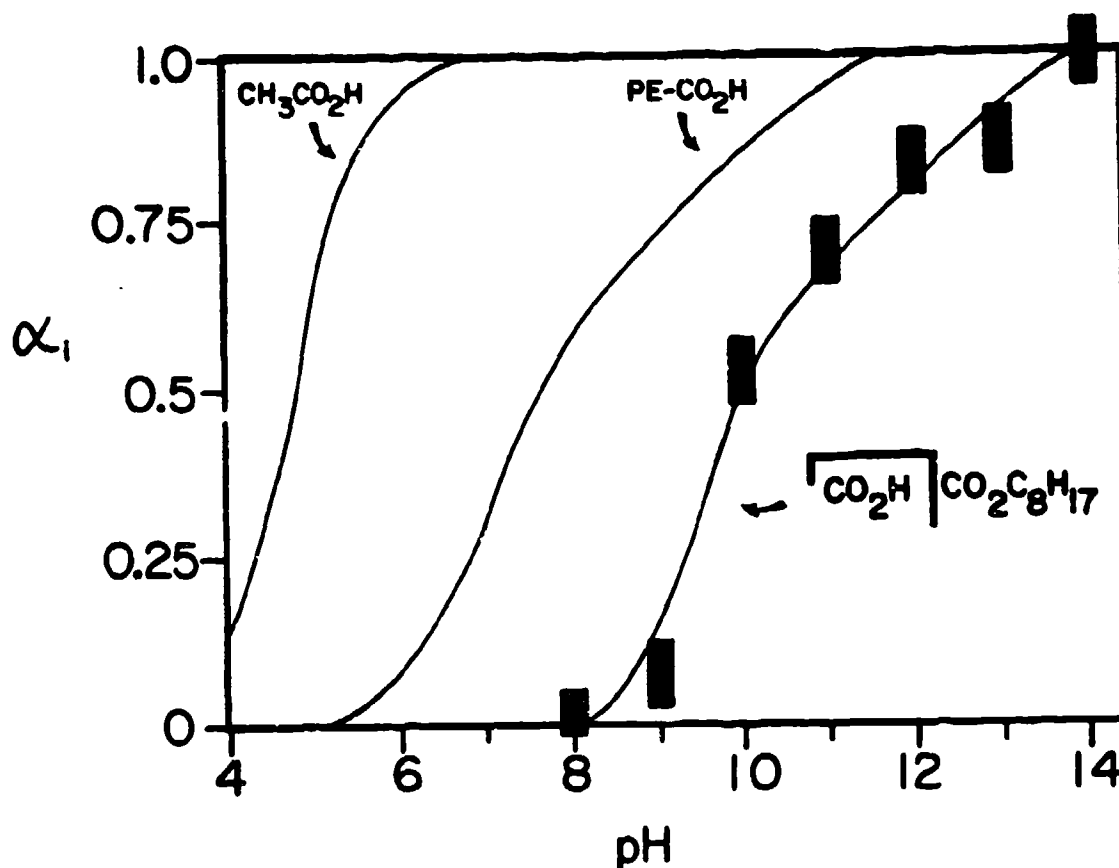
Figure 20. Ionization (α_i) as a function of pH determined by ATR-IR for PE-CO$_2$H and partially esterified PE-CO$_2$H using octanol. The points were determined from curves of the type in Figure 19 using eq 12 and 13.

Conclusions

The information summarized in this paper contributes to the resolution of a number of issues concerning the structure and reactivity of $PE-CO_2H$ and its derivatives, and more broadly to the study of organic surface chemistry.

i) <u>The functional groups in $PE-CO_2H/PE-CO_2R$ can be differentiated into subpopulations occupying the θ interphase and the sub-θ interphase</u>. The most immediate result of this research is its demonstration that the functional groups of $PE-CO_2H$ and its derivatives can be divided into two subsets: one influencing the wettability of these materials by water, and one <u>not</u> influencing the wettability but still accessible to hydroxide ion in the water. We propose that these subsets differ in their proximity to the polymer-water interface: those that influence wetting are in more intimate contact with the water than those that do not. This proposal immediately implies that the functionalized interface of $PE-CO_2H$ has finite thickness and is not a fully-exposed surface monolayer. We believe that van der Waals contact is necessary to influence wetting, but the issue of the nature of interactions between partially buried functionality and a contacting fluid phase is complex and unresolved, especially for systems such as $PE-CO_2H$, in which the interphase may swell and reconstruct in contact with water.

ii) <u>Approximately 30-50% of the functional groups in $PE-CO_2H$ occupy the θ interphase</u>. The functional groups in these systems belong to two different populations so far as their influence on wettability. What are the relative sizes of these populations? These relative populations clearly differ from system to system. We infer in the best-defined system so far examined--that obtained by partial base-catalyzed hydrolysis of $PE-CO_2CH_3$--that approximately 30-50% of the total $(CO_2CH_3)CO_2H$ groups occupy the θ interphase with water,

but that as few as 10% of the total groups may dominate the polymer-water interfacial free energy. The difference between estimates obtained from wetting using water at pH 1 and pH 13 are difficult to reconcile with a static model for the interface. We suggest that estimates at pH 1 reflect the composition of an unreconstructed interface more closely than those at pH 13. At the higher pH, reconstruction and/or swelling of the interphase may be driven by hydration of carboxylate ions.

iii) The behaviors of $PE-CO_2CH_3$ and $PE-CO_2C_8H_{17}$ are qualitatively different; these differences have no analogy in the behavior of soluble models such as $CH_3CO_2CH_3$ and $CH_3CO_2C_8H_{17}$. Esters of $PE-CO_2H$ and 1-octanol differ in several regards from esters with methanol: a smaller conversion of CO_2H to CO_2R groups in the θ interphase is sufficient to complete the accompanying change in wettability; complete esterification is much slower; hydrolysis of $PE-CO_2C_8H_{17}$ is also very slow. We suggest that all of these phenomena reflect the ability of the octyl esters to form a hydrophobic, low-polarity layer at the polymer-water interphase.

iv) The surface of $PE-CO_2H$ reconstructs on exposure to base and conversion of CO_2H to CO_2^- groups. Equation 5 is only approximately valid; "contact angle titration" should be considered a qualitative, rather than a quantitative technique. One clear and repeated inference from these studies is that the wetting of a number of materials derived from $PE-CO_2H$ are disproportionately sensitive to small concentrations of CO_2^- groups in the θ interphase (cf Figures 5,7,8,11,12,13,16,17); that is, that the influence of low concentrations of carboxylate ion on wettability is greater than would be extrapolated from the influence of this group at high concentrations. This point is made clear graphically by Figure 21, which plots $f_{\theta,pH\ 1}$ vs $f_{\theta,pH\ 13}$ for several of the systems examined. If, as implied by the assumptions in eq

Figure 21. Comparison of the portion of carboxylic acids present in the θ interphase detected by $\theta_{pH\ 1}$ and $\theta_{pH\ 13}$ during esterifications and hydrolyses of various surfaces. The portion of carboxylic acids is given by $f_{\theta(pH\ 1\ and\ 13)}$ for hydrolysis reactions and by $1-f_{\theta(pH\ 1\ and\ 13)}$ for esterification reactions. The curves represent data derived from f_θ vs time plots: A, PE-$CO_2C_8H_{17}$ $\rightarrow$ PE-CO_2H, Figure 13; B, PE-CO_2CH_3 $\rightarrow$ PE-CO_2H (OH^-), Figure 7; C, PE-$CO_2C_8H_{17}/CO_2H$ $\rightarrow$ PE-CO_2H, Figure 16; D, PE-CO_2CH_3 $\rightarrow$ PE-CO_2H (H^+), Figure 8; E, PE-COCl $\rightarrow$ PE-CO_2CH_3/CO_2H, Figure 11; F, PE-CO_2H $\rightarrow$ PE-CO_2CH_3, Figure 5; G, PE-CO_2H $\rightarrow$ PE-$CO_2C_8H_{17}$, Figure 12.

4 and 5, the functionalized interface is structurally stable and invariant to the medium in contact with it, and if the wettability of the surface (as measured by cos θ_a) is a linear function of the relative proportions of CO_2H groups (at pH 1) or CO_2^- groups (at pH 13) and CO_2CH_3 groups (at either pH), $f_{\theta,pH\ 1}$ should equal $f_{\theta,pH\ 13}$. Figure 21 indicates a systematic deviation: $f_{\theta,pH\ 1} \leq f_{\theta,pH\ 13}$. We have proposed to rationalize this deviation with the hypothesis that the functionalized interface can reconstruct to minimize the solid-liquid free energy, and that the extent of this reconstruction is more pronounced with interfaces containing CO_2^- groups than with those containing CO_2H groups.

Further evidence for this hypthesis comes from comparison of the curves in Figure 21. If reconstruction results in CO_2^- groups from the sub-θ interphase moving into the θ interphase, then samples with fewer CO_2^- groups in the sub-θ interphase should have less deviation between $f_{\theta,pH\ 1}$ and $f_{\theta,pH\ 13}$ due simply to the lower numbers of CO_2H (CO_2^-) species that can reconstruct. This hypothesis is supported by the experimental results where those surfaces with esters in the sub-θ interphase (PE $\overline{CO_2C_8H_{17}}$ CO_2H, $\underline{A}$; PE $\overline{CO_2CH_3}$ CO_2H, $\underline{B}$, $\underline{D}$) show less deviation than those surfaces with acid groups in the sub-θ interphase (PE $\overline{CO_2CH_3,CO_2H}$ CO_2H,CO_2CH_3 $\underline{E}$; PE $\overline{CO_2H}$ CO_2H; $\underline{C}$, $\underline{F}$, $\underline{G}$).

To conclude that the surface reconstructs is to bring eq 5 into question. Specifically, if the surface reconstructs, the fraction of CO_2H groups present in the θ interphase at pH 1 need not necessarily equal the fraction of CO_2^- groups present at pH 13: $x_{CO_2H,pH\ 1} \neq x_{CO_2^-,pH\ 13}$. This issue is of no relevance to several of the concerns of this paper--the differentiation of functional groups in PE-$CO_2H(R)$ into sets in distinct (θ and sub-θ) interphases, the accompanying inference of a functionalized

interphase of finite rather than monolayer thickness for PE-CO_2H in contact with water, the observation and rationalization of the differences in reactivities and properties of PE-CO_2CH_3 and PE-$CO_2C_8H_{17}$ and the contrast of these differences with the similar reactivities of $CH_3CO_2CH_3$ and $CH_3CO_2C_8H_{17}$ in solution--but it is important in discussing certain features of the acidity of CO_2H groups in the polymer interface. Our analyses of acidities are based either on straightforward analyses of ATR-IR spectra (for studies examining all of the functionalized interphase or the sub-θ interphase) or on an analysis of the variation in contact angle with pH (for studies focused on the θ interphase): the technique referred to here and in previous papers[3,4] as "contact angle titration." This procedure was derived on the assumption that the fraction of CO_2H (CO_2^-) moieties in the θ interphase of PE-CO_2H and derivatives is a constant independent of pH (i.e. that $x_{CO_2H} + x_{CO_2^-}$ is a constant in the θ interphase) and that the change in liquid/solid interfacial free energy with changes in pH depends linearly on the fraction α_i of carboxylic acid groups converted to carboxylate ions. The implication of this work is that the former assumption is incorrect, to some extent not presently quantified: that is, that $x_{CO_2H} + x_{CO_2^-}$ <u>increases</u> with pH.

What implication does the suggestion of an interphase for PE-CO_2H and its derivatives that is to some extent mobile and reconstructable carry for the accuracy of acidity data obtained by contact angle titration? A detailed answer to this question will require research beyond that described in this paper. We note, however, that data obtained by contact angle titration have been compared in a number of systems with data obtained using ATR-IR and potentiometric titration, and the results from the three techniques have been in good agreement.[3] Thus, the curves of α_i vs pH given in Figure 18 are probably qualitatively correct and comparable from system to system, but the

technique in general may suffer from a common systematic error when the acidity of sub-θ interphase groups is significantly different from the acidity of θ interphase groups.

v) <u>The acidities of CO_2H groups in PE-CO_2H and its derivatives are</u> <u>determined primarily by the dielectric constant of the interface. Charge-</u> <u>charge interactions are significant, but of secondary importance.</u> The CO_2H groups in both the θ and sub-θ interphases of PE-CO_2H and its partially esterified forms are significantly less acidic (that is, ionize at higher values of bulk solution pH) than simple alkane carboxylic acids in solution. The CO_2H groups in PE-CO_2H also ionize over a broader range of pH than would a simple monoprotic acid. We infer from the studies reported here that the shift to lower acidity reflects primarily a low polarity for the interfacial region. This inference is in agreement with studies of the interface carried out using a fluorescent reporter group (dansyl) that is sensitive to microscopic polarity.[4] The origin of the apparent width of the titration curves is still unclear. The data given here favor an interpretation based on charge-charge interaction between CO_2^- groups (that is, an interpretation in which PE-CO_2H is considered a polybasic acid with significant interaction between CO_2^- groups) rather than one requiring a distribution of non-interacting $CO_2H(CO_2^-)$ groups with a range of values of p$\underline{K}_a$. A previous study demonstrating no salt effect on the ionization of CO_2H groups in the θ interphase[3] can be reconciled with the suggestion of ion-ion interactions as the origin of the breadth of the titration curve only if it is assumed that ions are systematically excluded from the low polarity interfacial region.

A comparison of selected titration curves chosen to represent as closely as possible the behavior of CO_2H groups in the θ interphase, the sub-θ interphase, and the total functionalized interphase show relatively little

difference in terms of acidity (Figure 22). A larger difference in acidity

occurs when the polarity of the interphases is lowered by partial conversion

of CO_2H to $CO_2C_8C_{17}$ groups.

    vi) <u>The influence of the sub-θ interphase on groups in the θ interphase</u>

<u>in systems examined so far has reflected coulombic interactions and</u>

<u>penetration of the sub-θ groups into the θ interphase on derivatization.</u> The

importance of interactions between groups in the sub-θ and θ interphases

depends on the structures involved; from our limited studies, steric and

electrostatic effects both seem to be important. Thus, for example, the

ionization of CO_2H groups in the θ interphase appears to be influenced

electrostatically by exchange of CO_2CH_3 for CO_2H/CO_2^- groups in the sub-θ

interphase and is strongly influenced sterically and electrostatically by the

exchange of $CO_2C_8H_{17}$ for CO_2H/CO_2^- groups in this interphase. The origin of

this steric influence is probably penetration into the θ interphase of 1-octyl

chains on ester moieties in the sub-θ interphase. This observation leads to

the physically reasonable conclusion that the larger the groups incorporated

into the functionalized interphase, the thicker must be the layer included in

considering the structure of the θ interphase.

    vii) <u>The functionalized interphase(s) of PE-CO$_2$H has a thickness of</u>

<u>∿1 nm.</u> Combination of the information provided in this paper with that

obtained previously[3,4] begins to provide a useful level of detail to

considerations of the structure of the oxidatively functionalized interface of

PE-CO_2H. Some of this detail is clearly inferential, and requires further

experimental investigation. It is nonetheless useful in guiding research

based on PE-CO_2H as a model substrate with which to study the physical organic

chemistry of polymer surfaces.

Figure 22. Plots of extent of ionization (α_i) as a function of pH for acetic acid in solution, the θ interphase of PE-CO_2H determined by contact angle titration,[3] the total (θ + sub-θ) interphase of PE-CO_2H determined by IR,[3] the sub-θ interphase of PE-CO_2H partially esterified with octanol determined by IR, and the sub-θ interphase of PE-CO_2H determined by subtracting the θ interphase contribution from the total interphase curve. This subtraction assumed that the θ interphase comprised 30% of the total interphase (i.e.,

$$\alpha_{i_{(\text{sub }\theta)}} = 1.43 \left(\alpha_{i_{(\text{Total})}}\right) - 0.43 \left(\alpha_{i_{(\theta)}}\right)).$$

Approximately 30-50% of the functional groups in the interface can influence wetting and are thus either in direct van der Waals contact with the wetting liquid or otherwise strongly interacting with it. The upper end of this range--50%--is derived from experiments involving solutions at high pH and probably reflects an interphase that has to some extent reconstructed to maximize exposure of CO_2^- groups to the water. The polarity of the interphase is low ($\epsilon \sim 6-10$).[4] The apparent acidities of CO_2H groups in both the θ and sub-θ interphases are relatively low: $p\underline{K}_{1/2} \sim 7.5$. This low acidity is apparently due primarily to the low polarity of the interphase, and the accompanying energetic difficulties in creating and solvating a CO_2^- anion in it. The titration curve for the θ interphase CO_2H groups is appreciably broader than that for a monocarboxylic acid in solution. The relative contributions of charge-charge interactions and of differences in local polarities to this width remain unresolved. We have not been able to measure the thickness of the functionalized interphases directly, but the observation that incorporation of 1-octyl groups into either the θ or sub-θ interphase strongly influences the other suggests that these interphases have thicknesses comparable in size to a C_8 chain: that is, ~ 1 nm. We suggest that the functionalized interface is thus very thin.

viii) <u>New Materials: Thin-film Ion Exchange Resins</u>. The ability to manipulate the characteristics of the interphases of $PE-CO_2H$ by synthetic modification makes it possible to prepare a number of new types of materials. For example, $PE-CO_2C_8H_{17}$ is appreciably more hydrophobic than is unfunctionalized polyethylene itself, even though it has a high concentration of ester groups within angstroms of the polymer-water interface. Materials prepared by selective esterification of CO_2H groups in the θ interphase--e.g. $PE\overline{CO_2H}CO_2CH_3$ and $PE\overline{CO_2H}CO_2C_8H_{17}$--have the remarkable properties that their

constituent carboxylic acid moieties seem to have no direct contact with a contacting aqueous phase (the contact angle of water on these systems is independent of pH, and, at least for PE $\overline{CO_2H}$ $CO_2C_8H_{17}$ is that expected for a hydrocarbon-water interface) yet are completely accessible to hydroxide ion in aqueous solution and display titration behavior similar to that of the CO_2H groups of unmodified PE-CO_2H. These materials should thus be considered as a new class of very thin film ion exchange resins whose wetting characteristics can be varied independently through synthetic control of the thin layer constituting the θ interphase. We will describe a number of other new materials derived from PE-CO_2H and other surface-functionalized polymers in subsequent publications.

Experimental Section

General Procedures. Solvents and reagents were commercially obtained
and were analytical reagent grade. These were used as received. Values of pH
were determined by using a Cole Parmer 5995 pH meter with a Cole Parmer R5991-
81 electrode. Temperatures were not controlled and thus are accurate to ±2 °C
(the fluctuation in the laboratory temperature during the experiments). In
all of the procedures listed below, "rinsing" of the polyethylene samples
involved holding the corner of the sample with tweezers and gently moving the
sample through the liquid (~100 mL) for 10-20 sec. After this manipulation,
the samples were allowed to soak in the liquid for 1-3 min before being
removed from it. Once prepared, the surface properties of samples of PE-CO_2H
are stable on storage at room temperature and gentle manipulation.[3] The films
are handled using tweezers. Mechanical stress of the type experienced by the
film in the local area of contact with the tweezers does change wetting
characteristics. The modest stresses involved in flexing the film do not,
however, seem to do so. Thus, no particular precautions are required to avoid
mechanical deformation and stress during routine handling of the sample.

Contact Angle Measurements. Contact angles were determined on a Ramé-
Hart Model 100 contact angle goniometer equipped with an environmental chamber
by estimating the tangent normal to the drop at the intersection between the
sessile drop and the surface. These were determined 5-20 seconds after
application of the drop. The humidity in the chamber was maintained at 100%
by filling the wells in the sample chamber with distilled water. The
temperature was not controlled and varied betwen 20 and 25 °C. The volume of
the drop used was always 1 µL. Polyethylene samples were cut to a size of 0.5
x 2 cm and attached by the back of the sample to a glass slide using two-sided
Scotch tape to keep the sample flat. All reported values are the average of

at least eight measurements taken at different locations on the film surface and have a maximum error of the mean of ±3°. The buffers used were 0.05 M: pH 1, 0.1 N HCl; pH 2, maleic acid; pH 3, tartaric acid; pH 4, succinic acid; pH 5, acetic acid; pH 6, maleic acid; pH 7 and pH 8, HEPES; pH 9 and pH 10, CHES; pH 11, γ-aminobutyric acid; pH 12, phosphate; pH 13, 0.1 N NaOH. We have substituted other buffers with no significant differences in the results. For example, at pH 8, we have substituted phosphate, MOPS, HEPES, TAPS, TRIS, and triethanolamine with no significant changes in θ_a.[3]

ATR-IR. Samples were cut to the size of the KRS-5 crystal (45°, 50 x 20 x 2 mm) used and were equilibrated at the desired pH for 1 min. The films were removed and blotted with filter paper which had previously been equilibrated at the particular pH and dried.[3] The films were then dried in vacuum (0.01 torr) for 30 min before being placed in contact with the crystal. Rectangular pieces of thin cardboard the same size as the films were inserted between the films and the steel sample holder to distribute the pressure on the film evenly. Transmission spectra were obtained on a Perkin Elmer Model 598 spectrometer and converted directly to absorption spectra, by computer, for quantification. To account for differences in absorption due to slightly different degrees of contact between the polyethylene sample and the KRS-5 reflection element the absorbance peaks were always quantified relative to other peaks in the spectrum. In determining the ionization of the carboxylic acids at a given pH, for example, only the relative integrated absorbances at 1560 cm^{-1} (CO_2-) and 1710 cm^{-1} (CO_2H) were considered.

Polyethylene (PE-H). Low density biaxially blown polyethylene film (100 μm thick, ρ = 0.92) was a gift from Flex-O-Glass Inc (Flex-O-Film DRT-600B). The film was cut into 10 x 10 cm squares. These were extracted by suspending the film in refluxing CH_2Cl_2 for 24 h to remove antioxidants and

other film additives.[3] All samples were dried under vacuum (20 °C, 0.01 torr, 4 h) or air (4 h) prior to oxidation to remove any residual solvent. In all cases, experiments were performed on the side of film facing the inside of the stock roll.

Polyethylene Carboxylic Acid (PE-CO$_2$H). PE-H was oxidized by floating on H$_2$SO$_4$/H$_2$O/CrO$_3$ (29/42/29; w/w/w) at 72 °C for 60 sec. The samples were rinsed four times in distilled water, once in acetone, dried in air for 1 h and stored under dry argon or air in plastic petri dishes. The samples had a peak in the ATR-IR spectrum at 1710 cm^{-1}.

PE-CO$_2$R. Esters were made by soaking PE-CO$_2$H in the appropriate alcohol (300 mL) containing sulfuric acid (45 mL) for 5 days at 40 °C (1 day for methanol). The samples were then rinsed in the same alcohol twice, water twice, methanol once and air dried. The samples were stored in petri dishes in the air. The samples all had a new ATR-IR peak at 1740 cm^{-1} (CO$_2$R) and no longer had a peak at 1560 cm^{-1} (CO$_2^-$) after treatment with 0.1 N NaOH.[3,4] Films made of the longer esters (hexyl, octyl) smelled strongly of alcohol after work-up. Soaking of these samples in acetone or methanol for 3 days eliminated the odor but did not otherwise influence the properties of the film (θ_a, ATR-IR of carbonyl region).

CH$_3$CO$_2$CH$_3$. Acetic acid (10 mL) was added to 300 mL of CH$_3$OH containing 45 mL H$_2$SO$_4$ and 40 °C. After the desired time (∿1 min) a 1-mL sample was removed and neutralized in 1 mL of Fisher pH 7 buffer concentrate (undiluted), containing 3-pentanone as a standard, and stored on ice. Samples (1 µL) were analyzed by GC (Supelco SP 2100 column, room temp). Elution times were 70 and 226 sec for the 3-pentanone and the methyl acetate, respectively. The ratio of these two molecules was used to follow the esterification reaction.

PE-COCl. PE-CO$_2$H was soaked in anhydrous ether saturated with PCl$_5$ (saturated by letting solid PCl$_5$ sit in the solution for 3 h prior to, and during, reaction). After 1 h the film was removed and transferred directly into the water/methanol mixtures to form mixed acid/ester surfaces. The samples were removed after 15 minutes and rinsed in acetone (4 times). The samples were dried in air and stored in petri dishes.

CH$_3$CH$_2$CH$_2$CO$_2$H/CO$_2$CH$_3$. Butyric acid chloride (10 mL) was mixed with 3-pentanone (10 mL). Portions of this mixture (200 µL) were removed and added to the appropriate water/methanol mixture (100 mL). Aliquots (1 µL) were removed from each and analyzed by GC using a Supelco SP2100 column at room temp. Elution times were 220 and 300 sec for the 3-pentanone and methyl butyrate, respectively. The ratio of these two molecules was used to follow the reaction (i.e. the relative proportion of ester compared to acid).

Base-Catalyzed Hydrolysis of PE-CO$_2$R. Hydrolyses in base were carried out by floating PE-CO$_2$R (ester side down) on the surface of 1 N NaOH at 20 ± 2 °C for the specified length of time. The films were rinsed in water 3 times, acetone once, and air dried. Rates for soluble analogs were determined both experimentally and from the second-order rate constants published in the literature.[25] Experimentally, a mixture of methyl acetate (0.5 mL) and 3-pentanone (0.5 mL) was added to 100 mL of 1.0 N NaOH with vigorous stirring. At given intervals samples (1 mL) were removed and added to 3 mL of Fisher pH 7 buffer concentrate (undiluted) and stored on ice. These mixtures were analyzed by injecting 3 uL aliquots into a GC (Supelco SP 2100 column, room temp) and monitoring the ester and ketone peaks. Elution times were 80 and 230 sec for the methyl acetate and 3-pentanone, respectively. The relative size of the methyl acetate peak was used to follow the reaction. After 10 seconds, less than 5% of the initial ester remained, indicating a

half life of less than 5 seconds. This value is lower than the literature value derived from rate constants ($t_{1/2} \approx 8$ sec) and thus the literature values quoted in this paper should be considered lower limits to the reaction rate for the conditions employed here (1 N NaOH).

Acid-Catalyzed Hydrolysis of PE-CO$_2$CH$_3$. Hydrolysis was carried out by floating PE-CO$_2$CH$_3$ (ester side down) on the surface of 50% (w/w) H$_2$SO$_4$ at 25 ± 2 °C for the specified time. The film was rinsed 4 times in water, once in acetone, and air dried. Literature values for the hydrolysis rate were determined from the pseudo-first-order rate constants established under identical conditions.[26]

References

1) This work was supported in part by the Office of Naval Research and by the National Science Foundation through grants to the Harvard Materials Research Laboratory.

2) IBM Predoctoral Fellow in Polymer Chemistry, 1984-1986.

3) Holmes-Farley, S. R.; Reamey, R. H.; McCarthy, T. J.; Deutch, J.; Whitesides, G. M. Langmuir 1985, 1, 725.

4) Holmes-Farley, S. R.; Whitesides, G. M. Langmuir 1986, 2, 266.

5) Rasmussen, J. R.; Stedronsky, E. R.; Whitesides, G. M. J. Am. Chem. Soc. 1977, 99, 4736.

6) Rasmussen, J. R.; Bergbreiter, D. E.; Whitesides, G. M. J. Am. Chem. Soc. 1977, 99, 4746.

7) Adamson, A. W. "Physical Chemistry of Surfaces"; Wiley: New York, 1982. Vold, R. D.; Vold, M. J. "Colloid and Interface Chemistyry"; Addison-Wesley: Reading, MA, 1983.

8) Jaycock, M. J.; Parfitt, G. D. "Chemistry of Interfaces"; John Wiley and Sons: New York, 1981.

9) Good, R. J.; Stromberg, R. R. "Surface and Colloid Science"; Plenum: New York, 1979; Vol. 11.

10) de Gennes, P. G. Rev. Mod. Phys. 1985, 57, 827.

11) Joanny, J. F.; de Gennes, P. G. J. Chem. Phys. 1984, 81, 552.

12) Kaelble, D. H. "Physical Chemistry of Adhesion"; Wiley: New York, 1971; p 170.

13) Gould, R. F., Ed. Advan. Chem. Ser. 1964, 43.

14) Schwartz, L. W.; Garoff, S. Langmuir 1985, 1, 219.

15) Schwartz, L. W.; Garoff, S. J. Coll. Int. Sci. 1985, 106, 422.

16) Cherry, B. W. "Polymer Surfaces"; Cambridge University Press: Cambridge, 1981.

17) Woodruff, D. P. "The Solid-Ligand Int rface"; Cambridge University Press: Cambridge, 1981.

18) Fortes, M. A. J. Chem. Soc., Faraday Trans. 1 1982, 78, 101.

19) Malev, V. V.; Gribanova, E. V. Dokl. Akad. Navk. SSSR 1983, 272, 413.

20) Wolfram, E.; Faust, R. Anales Universitatie Scientiarum Budapest 1980, 151.

21) Baszkin, A.; Ter-Minassian-Saraga, L. J. Coll. Int. Sci. 1973, 43, 190.

22) Pomeau, Y.; Vannimenus, J. Coll. Int. Sci. 1985, 104, 477.

23) Smith, L. M.; Bowman, L.; Andrade, J. D. Proceedings of the Durham England Conference on Biomedical Polymers 1982.

24) Evidence for the hypothesis that functional groups must be within a few angstroms of the surface in order to influence wetting comes from two sources. In the first system, consisting of monolayers of alkyl sulfides of the form $CH_3(CH_2)_nS(CH_2)_mCO_2H$ adsorbed onto clean gold surfaces, we have found that the wetting of the monolayer by water was only influenced by the carboxylic acid group if it was within 1 nm of the surface. Specifically, if m was shorter than n, the carboxylic acid was constrained to lie below the surface. When n-m was greater than 5, the wetting was similar to that observed for $CH_3(CH_2)_nS(CH_2)_mCH_3$, demonstrating that the carboxylic acid group was buried too deeply to influence wetting (B. Troughton, unpublished results). In the second system (consisting of a surface modified polyethylene film with hydroxy groups on its surface, $PE-CH_2OH$), we found that heating the sample allowed the hydroxy groups to diffuse into the polymer. After heating, the sample had wetting properties similar to unmodified polyethylene;

thus, the hydroxy groups are buried too deeply to influence wetting. After treating this thermally reconstructed material with species such as $(CF_3CO)_2O$ to acylate the hydroxyl groups, the wetting properties changed markedly. Thus, "extending the reach" of the hydroxy group by less than 1 nm changes the wetting properties significantly, although the hydroxy groups themselves do not influence wetting (S. R. Holmes-Farley, unpublished results). We note that the maximum depth from which functional groups can influence wetting is expected to depend strongly on the nature of the material above the groups, particularly on the degree to which the intervening material is swollen by solvent.

25) Smith, L.; Olsson, H. Z. Phys. Chem. 1925, 118, 99; Olsson, H. Z. Phys. Chem. 1925, 118, 107.

26) Yates, K.; McClelland, R. A. J. Am. Chem. Soc. 1967, 89, 2686.

27) Jones, R. N. A.; Thomas, J. D. R. J. Chem. Soc. (B) 1966, 661.

28) Hammond, G. S.; Hogle, D. H. J. Am. Chem. Soc. 1955, 77, 338.

29) Laskowski, M.; Scheraga, H. A. J. Am. Chem. Soc. 1954, 76, 6305.

30) Albert, A.; Serjent, E. P. "The Determination of Ionization Constants"; University Press: Cambridge, 1984, 35.

31) Clare, B. W.; Cook, D.; Ko, E. C. F.; Mac, Y. C.; Parker, A. J. J. Am. Chem. Soc. 1966, 88, 1911.

32) Bordwell, F. G. Pure Appl. Chem. 1977, 49, 963.

33) Hansch, C.; Leo, A.; Unger, S. H.; Kim, K. H.; Mikaitani, D.; Lien, E. J. J. Med. Chem. 1973, 16, 1207. Hansch, C.; Rockwell, S. D.; Jow, P. Y. C.; Leo, A.; Steller, E. E. J. Med. Chem. 1977, 20, 304.

34) Atkins, W. P. "Physical Chemistry"; Oxford University Press, Great Britain, 1978; p 316.

35) Gregor, H. P.; Frederick, M. J. Polym. Sci. 1957, 23, 454.

36) A similar phenomenon has been observed previously for PE⎤CO$_2$H⎡CH$_2$, the material obtained by thermal reconstruction of the surface of PE-CO$_2$H. This material has $\theta_{a(pH\ 5\ and\ pH\ 13)}$ = 103°--the value characteristic of unoxidized polyethylene--but the carboxylic acid groups below the θ interphase are still completely accessible to base (T. McCarthy, unpublished).

Captions

Figure 1. Ambiguities concerning influence of a functional group of (■) on wetting. A: On the surface (position 1) and in the interior of a planar solid (position 2). B: On the surface (1), on the wall (2) and at the bottom of a microcrack (3). C: In the outmost (1), middle (2) and base (3) of a solvent-swollen surface gel region.

Figure 2. Nomenclature used to describe the several interphase regions of PE-CO_2H and its derivatives.

Figure 3. Representative ATR-IR spectra of PE-CO_2H taken after treatment of the film with acid (pH 1) or base (pH 13) obtained during acid-catalyzed esterification of the carboxylic acid groups in methanol. The absorption at 1560 cm^{-1} is due to the CO_2^- group, and was the peak followed in determining the extent of reaction. The ester absorption occurs at 1740; the peak at 1710 includes both carboxylic acid and ketone groups.

Figure 4. Representative contact angles observed during acid-catalyzed esterification of PE-CO_2H in methanol. Points were taken at pH 1 (0.1 N HCl) to observe CO_2H groups, and at pH 13 (0.1 N NaOH), to observe CO_2^- groups. Esterifications were conducted in anhydrous methanol containing 13% H_2SO_4 at 40 °C. The height of the symbols representing the data points are indicative of the estimated error bars in all figures except 5, 7, 8, 13 and 17.

Figure 5.   <u>Top</u>: Progression of contact angle ($f_{\theta,\text{pH 1}}$, $f_{\theta,\text{pH 13}}$; eq 7), and

ATR-IR (f_{IR}; eq 1 and 2) from initial to final values during acid-

catalyzed esterification of PE-CO_2H to PE-CO_2CH_3 (derived from the

data in Figures 3 and 4). The data points for $f_{\theta,\text{pH 1}}$ and

$f_{\theta,\text{pH 13}}$ are the result of three different experiments.

Similarly, the open squares contain the data points for three

different ATR-IR experiments. In this figure, and in figures 7,

8, 13 and 17, the errors associated with the experiment are best

estimated from the data scatter and thus the individual data

points are drawn smaller than their estimated error for clarity.

<u>Bottom</u>: The relationship between f_{θ} (pH 1 and pH 13) and f_{IR}

based on the data in the upper portion of the figure.

Figure 6.   First-order kinetic plots for $f_{\theta,\text{pH 1}}$, $f_{\theta,\text{pH 13}}$ and f_{IR} for acid-

catalyzed esterification. For comparison, the plot also includes

data for the conversion of acetic acid to methyl acetate under the

same conditions (followed by GC).

Figure 7.   Progression of f_{θ} and f_{IR} from initial to final values during

base-catalyzed hydrolysis of PE-CO_2CH_3 in 1 N NaOH at T = 20 °C.

The f_{θ} (pH 1 and pH 13) data points represent three different

experiments. Similarly, the open squares represent three

different ATR-IR experiments.

Figure 8.   Progression of f_{θ} and f_{IR} from initial to final values during

acid-catalyzed hydrolysis of PE-CO_2CH_3 in 50% (w/w) H_2SO_4,

T = 25 °C.

Figure 9.   First-order kinetic plots for $f_{\theta,\text{pH 1}}$, $f_{\theta,\text{pH 13}}$ and f_{IR} from the

data of Figure 7. For comparison, the plot includes data for

homogeneous hydrolysis of $CH_3CO_2CH_3$ under the same conditions.[25]

Figure 10. Kinetic plots for $f_{\theta,pH\ 1}$, $f_{\theta,pH\ 13}$ and f_{IR} from the data of Figure 8. For comparison, the plot includes data for homogeneous hydrolysis of $CH_3CO_2CH_3$ under the same conditions.[26]

Figure 11. Progression of f_θ (pH 1 and pH 13) and f_{IR} for reaction of PE-COCl with water-methanol mixtures. The figure includes data for butyric acid chloride under the same conditions (determined by GC).

Figure 12. <u>Top</u>: Progression of $\theta_{pH\ 1}$ and $\theta_{pH\ 13}$ for the acid-catalyzed esterification of PE-CO_2H in octanol (300 mL) containing H_2SO_4 (75 mL) at 40 °C. <u>Bottom</u>: Progression of $f_{\theta,pH1}$, $f_{\theta,pH13}$ and f_{IR} for the acid-catalyzed esterification of PE-CO_2H. The values for f_θ were determined from the data in the upper portion of the figure by using equation 7.

Figure 13. Progression of $f_{\theta,pH\ 1}$, $f_{\theta,pH\ 13}$, and f_{IR} for the base-catalyzed hydrolysis of PE-$CO_2C_8H_{17}$ in 1 N NaOH at 20 °C. The curve for the base-catalyzed hydrolysis of PE-CO_2CH_3 determined by IR (Figure 7) is shown for comparison.

Figure 14. Schematic illustrations of: A) a partially esterified PE-CO_2H surface using octanol; B) a partially esterified PE-CO_2H surface using methanol; C) a partially hydrolyzed PE-$CO_2C_8H_{17}$ surface; D) a partially hydrolyzed PE-CO_2CH_3 surface.

Figure 15. First-order kinetic plots for f_θ and f_{IR} for the base-catalyzed hydrolysis of PE-$CO_2C_8H_{17}$ using the data in Figure 13. The values of f reached after $\sim$3 weeks in base (30,000 min) are indicated on the figure. Beyond this point, little reaction takes place up to >80,000 min.

Figure 16. Progression of $f_{\theta,pH\ 1}$ and $f_{\theta,pH\ 13}$ for a partially esterified sample of PE-CO$_2$H using octanol (Figure 13, log t = 2.0), similar to that shown in Figure 14. The curves of $f_{\theta,pH\ 1}$ for PE-CO$_2$CH$_3$ and PE-CO$_2$C$_8$H$_{17}$ are shown for comparison.

Figure 17. <u>Upper</u>: Plots of θ_a vs pH for esterification of PE-CO$_2$H. The plot on the right gives the fraction of total carboxyl groups present as carboxylic acids (x_{CO_2H}, eq 11, derived from f_{IR}). The dotted lines in the plots give the values taken as $\alpha_i = 0$, $\alpha_i = 0.5$ (p$K_{1/2}$) and $\alpha_i = 1.0$. <u>Middle</u>: Plots of θ_a vs pH for surfaces made by reacting PE-COCl with CH$_3$OH/H$_2$O mixtures. <u>Bottom</u>: Plots of θ_a vs pH for base-catalyzed hydrolysis of PE-CO$_2$CH$_3$.

Figure 18. <u>Upper</u>: Plots of the extent of ionization α_i of the CO$_2$H groups present on the surface of PE CO$_2$H CO$_2$CH$_3$ at different extents of esterification of PE-CO$_2$H. The curves were determined from the data in Figure 17 using eq 10. The numbers attached to the lines represent the fraction of the mixture of CO$_2$H and CO$_2$CH$_3$ groups present as CO$_2$H (x_{CO_2H}, eq 11). Continuous lines represent surfaces with only CO$_2$H groups in the θ interphase ($\theta_{pH\ 1} \approx 55°$). Dashed lines represent surfaces with roughly equal numbers of methyl ester and acid groups in the θ interphase ($\theta_{pH\ 1} \approx 73°$). Dotted lines represent those samples with just enough carboxylic acid groups in the θ interphase to obtain an accurate contact angle titration ($\theta_{pH} = 90°$; ester/acid ~ 5 in θ interphase). <u>Middle</u>: Same as upper portion for surfaces made by reaction of PE-COCl with water/methanol mixtures. <u>Bottom</u>: Same as upper portion for surfaces made by base-catalyzed hydrolysis of PE-CO$_2$CH$_3$.

Figure 19. Types of curves used in ATR-IR determinations of α_i vs pH for PE-CO$_2$H and the sub-θ interphase of partially esterified PE-CO$_2$H using octanol (Figure 12, lot t = 3.2).

Figure 20. Ionization (α_i) as a function of pH determined by ATR-IR for PE-CO$_2$H and partially esterified PE-CO$_2$H using octanol. The points were determined from curves of the type in Figure 19 using eq 12 and 13.

Figure 21. Comparison of the portion of carboxylic acids present in the θ interphase detected by $\theta_{pH\ 1}$ and $\theta_{pH\ 13}$ during esterifications and hydrolyses of various surfaces. The portion of carboxylic acids is given by $f_{\theta(pH\ 1\ and\ 13)}$ for hydrolysis reactions and by $1-f_{\theta(pH\ 1\ and\ 13)}$ for esterification reactions. The curves represent data derived from f_θ vs time plots: A, PE-CO$_2$C$_8$H$_{17}$ $\rightarrow$ PE-CO$_2$H, Figure 13; B, PE-CO$_2$CH$_3$ $\rightarrow$ PE-CO$_2$H (OH$^-$), Figure 7; C, PE-CO$_2$C$_8$H$_{17}$/CO$_2$H $\rightarrow$ PE-CO$_2$H, Figure 16; D, PE-CO$_2$CH$_3$ $\rightarrow$ PE-CO$_2$H (H$^+$), Figure 8; E, PE-COCl $\rightarrow$ PE-CO$_2$CH$_3$/CO$_2$H, Figure 11; F, PE-CO$_2$H $\rightarrow$ PE-CO$_2$CH$_3$, Figure 5; G, PE-CO$_2$H $\rightarrow$ PE-CO$_2$C$_8$H$_{17}$, Figure 12.

Figure 22. Plots of extent of ionization (α_i) as a function of pH for acetic acid in solution, the θ interphase of PE-CO$_2$H determined by contact angle titration,[3] the total (θ + sub-θ) interphase of PE-CO$_2$H determined by IR,[3] the sub-θ interphase of PE-CO$_2$H partially esterified with octanol determined by IR, and the sub-θ interphase of PE-CO$_2$H determined by subtracting the θ interphase contribution from the total interphase curve. This subtraction assumed that the θ interphase comprised 30% of the total interphase (i.e., $\alpha_{i(sub\ \theta)} = 1.43\ (\alpha_{i(Total)}) - 0.43\ (\alpha_{i(\theta)})$).

APPENDIX
ENCLOSURE NUMBER 3
CONTRACT DATA REQUIREMENTS LIST
INSTRUCTIONS FOR DISTRIBUTION
ARPA/ONR

CONTRACT NUMBER: N00014-85-K-0898
ATTACHMENT NO.: 1

MINIMUM DISTRIBUTION OF TECHNICAL REPORTS

ADDRESSEE	DODAAD CODE	NUMBER OF COPIES	
		UNCLASSIFIED/UNLIMITED	UNCLASSIFIED/LIMITED AND CLASSIFIED
Director, Advanced Research Projects Agency 1400 Wilson Boulevard Arlington, Virginia 22209 ATTN: Program Management	HX1241	2	2
Scientific Officer	N00014	3	3
Administrative Contracting Officer	N66016	1	1
Director, Naval Research Laboratory, ATTN: Code 2627 Washington, D. C. 20375	N00173	6	1
Defense Technical Information Center Bldg. 5, Cameron Station Alexandria, Virginia 22314	S47031	12	2

One (1) copy of each technical report resulting from work performed in the area of tactical technology shall be sent to:

	DODAAD CODE
TACTEC Battelle Memorial Institue 505 King Avenue Columbus, Ohio 43201	79986

MINIMUM DISTRIBUTION OF REPORTS WHICH ARE NOT TECHNICAL REPORTS

ADDRESSEE	DODAAD CODE	NUMBER OF COPIES	
		UNCLASSIFIED/UNLIMITED	UNCLASSIFIED/LIMITED AND CLASSIFIED
Director, Advanced Research Projects Agency 1400 Wilson Boulevard Arlington, Virginia 22209 ATTN: Program Management	HX1241	2	2
Scientific Officer	N00014	3	3
Administrative Contracting Officer	N66016	1	1

If the Scientific Officer directs, the Contractor shall make additional distribution of technical reports and such other reports as may be specified by the Scientific Officer in accordance with a supplemental distribution list provided by the Scientific Officer.